FOXO AND AUTOPHAGY CONTRIBUTE TO MECHANICAL VENTILATION-INDUCED ATROPHY AND CONTRACTILE DYSFUNCTION IN THE DIAPHRAGM

By

ASHLEY JOSLIN SMUDER

A DISSERTATION PRESENTED TO THE GRADUATE SCHOOL
OF THE UNIVERSITY OF FLORIDA IN PARTIAL FULFILLMENT
OF THE REQUIREMENTS FOR THE DEGREE OF
DOCTOR OF PHILOSOPHY

UNIVERSITY OF FLORIDA

2012

To my family and friends for their constant support and to the people who have played a significant role in my education

ACKNOWLEDGMENTS

First, I thank my mentor Dr. Scott Powers for his guidance and continuous support during my graduate education. Also, I commend my thesis committee members; Dr. Nihal Tümer, Dr. Thomas Clanton and Dr. Stephen Dodd for their direction and support. I thank Dr. Krista Vandenborne for giving me the opportunity to be involved with an National Institute of Health T32 training award. Of course I also wish to thank all the laboratory members who played a role in my achievements. Finally, I am thankful for my family and friends who share my life and career experiences.

TABLE OF CONTENTS

page

ACKNOWLEDGMENTS 4

LIST OF TABLES 8

LIST OF FIGURES 9

LIST OF ABBREVIATIONS 11

ABSTRACT 12

CHAPTER

1 INTRODUCTION 13

2 LITERATURE REVIEW 16

Overview of Ventilator-Induced Diaphragm Dysfunction 16
Diaphragm Response to Mechanical Ventilation 17
Mechanisms of MV-induced Diaphragmatic Dysfunction 18
Diaphragm contractile dysfunction 18
Diaphragm atrophy 18
Protein synthesis and degradation 19
Summary 23

3 MATERIALS AND METHODS 24

Experiment 1: Animals 24
Animal Model Justification 24
Animal Housing and Diet 24
Experimental Design 24
Packaging and Purification of Recombinant AAV Vectors 25
Animal Protocol 25
Statistical Analysis 26
Experiment 2: Animals 27
Animal Model Justification 27
Animal Housing and Diet 27
Experimental Design 27
Packaging and Purification of Recombinant AAV Vectors 27
Animal Protocol 28
Statistical Analysis 29
Experiment 3: Animals 29
Animal Model Justification 29
Animal Housing and Diet 29
Experimental Design 30

Packaging and Purification of Recombinant AAV Vectors 30
Animal Protocol 30
Statistical Analysis 32
General Methods 32
Histological Measures 32
Functional Measures 33
Biochemical Measures 34
Mitochondrial Measures 35

4 RESULTS 38

Experiment 1: Systemic Response to Mechanical Ventilation 38
Redox Balance 38
4-HNE 38
Mitochondrial Reactive Oxygen Species Emission 39
Diaphragm Function 39
Mitochondrial Function 39
Contractile Function 39
Diaphragm Structure 40
Proteolytic Activity 40
Calpain 40
Caspase-3 41
Ubiquitin-Proteasome System 41
Experiment 2: Systemic Response to MV 42
Redox Balance 42
4-HNE 42
Mitochondrial ROS 42
Diaphragm Function 43
Mitochondrial Function 43
Contractile Function 43
Diaphragm Structure 44
Cross-sectional Area 44
Electron Microscopy 44
Proteolytic Activity 44
Calpain 44
Caspase-3 45
Autophagy/Lysosomal System 45
Experiment 3: Systemic Response to MV 46
Diaphragm Structure 46
Autophagic/Lysosomal System 46
Autophagosome Initiation 46
Autophagosome Formation 47
Lysosomal Proteases 48

5 DISCUSSION 65

Overview of Principal Findings 65

Mechanical Ventilation-induced Induction of FOXO Transcription..... 65
FOXO Signaling Contributes to Ventilator-induced Diaphragm Dysfunction 66
MV-induced Induction of Autophagy..... 67
Autophagy Contributes to VIDD 68
FOXO and Autophagy 69
Conclusions and Future Directions 71

LIST OF REFERENCES 72

BIOGRAPHICAL SKETCH 77

LIST OF TABLES

Table page

4-1 Mitochondrial respiratory function in permeabilized fibers from diaphragm muscle obtained for experiment 1..... 50

4-2 Mitochondrial respiratory function in permeabilized fibers from diaphragm muscle obtained for experiment 2..... 55

LIST OF FIGURES

Figure page

3-1 Experimental animal design used to determine the effect of blocking FOXO transcription during MV on diaphragm function and activation of proteolytic pathways. 37

3-2 Experimental animal design used to determine the effect of blocking Atg5 activation during MV on diaphragm function and activation of proteolytic pathways. 37

4-1. The levels of 4 hydroxynonenal (4-HNE) were analyzed as an indicator of lipid peroxidation via western blotting for experiment 1. 49

4-2 Rates of hydrogen peroxide release (H_2O_2) release from permeabilized diaphragm muscle fibers for experiment 1. 49

4-3 Diaphragm force-frequency response (*in vitro*) of diaphragm samples for experiment 1. 51

4-4 Diaphragm muscle cross-sectional area for experiment 1. 51

4-5 Calpain activation in diaphragm was determined via Western blotting for experiment 1. 52

4-6 Caspase-3 activation in the diaphragm was determined via Western blotting for experiment 1. 52

4-7 Atrogin-1 was measured as a marker of FOXO activity for experiment 1. 53

4-8 MuRF1 was measured as a marker of FOXO activity for experiment 1. 53

4-9 The levels of 4 hydroxynonenal (4-HNE) were analyzed as an indicator of lipid peroxidation via western blotting for experiment 2. 54

4-10 Rates of hydrogen peroxide release (H_2O_2) release from permeabilized diaphragm muscle fibers for experiment 2. 54

4-11 Diaphragm force-frequency response (*in vitro*) of diaphragm samples for experiment 2. 56

4-12 Diaphragm muscle cross-sectional area for experiment 1. 56

4-13 Electron microscopy representative images of diaphragm muscle obtained from animals in experiment 2. 57

4-14 Calpain activation in diaphragm was determined via Western blotting for experiment 2. 57

4-15 Caspase-3 activation in the diaphragm was determined via Western blotting for experiment 2. 58

4-16 Beclin 1 was measured as a marker of the initiation of autophagosome formation for experiment 2. 58

4-17 Atg5 and Atg12 were analyzed as markers of elongation of the autophagosome for experiment 2. 59

4-18 Atg12-Atg5 complex expression was measured via Western blotting as a marker of autophagosome formation for experiment 2. 59

4-19 LC3 was measured as a marker of elongation and formation of the autophagosome for experiment 2. 60

4-20 LC3 accumulation was examined in diaphragm muscle cross-sections for experiment 2. 60

4-21 Electron microscopy representative images images of diaphragm muscle obtained from animals in experiment 3 61

4-22 Beclin 1 was measured as a marker of the initiation of autophagosome formation for experiment 3. 61

4-23 Atg4 was measured as a marker of the formation of the autophagosome for experiment 3. 62

4-24 Atg7 was measured as a marker of the formation of the autophagosome for experiment 3. 62

4-25 LC3 was measured as a marker of elongation and formation of the autophagosome for experiment 3. 63

4-26 LC3 accumulation was examined in diaphragm muscle cross-sections for experiment 3. 63

4-27 Cathepsin L was measured as a marker of increased degradation by the lysosomal proteolytic system for experiment 3. 64

LIST OF ABBREVIATIONS

4-HNE	4-Hydroxynoneal
ATG	Autophagy gene
CSA	Cross-sectional area
dn	Dominant negative
MV	Mechanical ventilation
PaO_2	Partial pressure of oxygen
$PaCO_2$	Partial pressure of carbon dioxide
RCR	Respiratory control ration
ROS	Reactive oxygen species
SBDP	Spectrin breakdown product
VIDD	Ventilator-induced diaphragm dysfunction

Abstract of Dissertation Presented to the Graduate School
of the University of Florida in Partial Fulfillment of the
Requirements for the Degree of Doctor of Philosophy

FOXO AND AUTOPHAGY CONTRIBUTE TO MECHANICAL VENTILATION-INDUCED ATROPHY AND CONTRACTILE DYSFUNCTION IN THE DIAPHRAGM

By

Ashley Joslin Smuder

May 2012

Chair: Scott K. Powers
Major: Health and Human Performance

Mechanical ventilation (MV) is used to mechanically assist or replace spontaneous breathing in patients with respiratory failure. The removal of MV from patients is termed “weaning” and problems in weaning occur frequently. Importantly, weaning difficulties are attributed to diaphragm weakness caused by atrophy and contractile dysfunction. It is established that oxidative stress in the diaphragm is an important contributor to MV-induced diaphragm weakness. However, the signaling pathways that connect reactive oxygen species (ROS) to MV-induced diaphragm weakness remain unknown. In this regard FOXO and autophagy signaling have been shown to contribute to disuse-induced skeletal muscle atrophy. Therefore, the goal of these experiments was to determine the contribution of FOXO activity as well as autophagy to MV-induced diaphragm weakness. To test this we used an animal experimental model of MV and a loss of function approach using a dominant negative (dn) FOXO plasmid and a dnAtg5 plasmid to knockdown either FOXO or autophagy. Specifically, administration of either the dnFOXO or the dnATG5 plasmid during MV resulted in only partial protection of diaphragm function following MV. Therefore, we conclude that both FOXO transcription and autophagy signaling play a role in MV-induced diaphragm dysfunction.

CHAPTER 1
INTRODUCTION

Mechanical ventilation (MV) is a life-saving measure for patients in respiratory failure. Respiratory drug overdose, surgery and spinal cord injury are among the common clinical conditions that require MV (12, 17). The withdrawal of MV from patients is referred to as “weaning” and problems in weaning from MV are common (~30% of patients) (23). In fact, weaning difficulties account for almost half of the time spent on the ventilator (11). In this regard, there is accumulating evidence that weaning problems are linked to inspiratory muscle dysfunction which results in the inability of the respiratory muscles to maintain adequate ventilation. Specifically, our laboratory has shown that respiratory muscle weakness produced by prolonged MV is due to diaphragmatic atrophy and contractile dysfunction [collectively referred to as ventilator-induced diaphragm dysfunction (VIDD)] (39, 40, 50, 52). Therefore understanding the cellular mechanisms responsible for VIDD is important.

In this regard, VIDD is primarily due to increased proteolysis (i.e. breakdown of muscle proteins) (26, 29, 51). This MV-induced proteolysis in the diaphragm occurs via a highly coordinated interaction between four major proteolytic systems: 1) calpains; 2) caspases; 3) ubiquitin-proteasome system; and 4) autophagic/lysosomal system. Our laboratory has shown the importance of the calpain and caspase-3 proteolytic systems. However, the exact role that the ubiquitin-proteasome system and the lysosomal system play during VIDD has not been elucidated.

The ubiquitin-proteasome degradation pathway is active after ubiquitin covalently binds to protein substrates and marks them for degradation. Atrogin-1/MAFbx and MuRF1 are both important proteins in this process. Specifically, during conditions of

muscle wasting, the transcription factor FOXO is dephosphorylated and translocated to the nucleus which leads to the induction of atrogin-1 and MuRF1 and subsequent muscle protein breakdown by the proteasome (18, 46). In addition to contributing to proteasome-induced muscle atrophy, FOXO activation can also increase the transcription of numerous proteins important for autophagy. Therefore, FOXO can independently control two major systems of protein degradation. However, the role of FOXO in VIDD is currently unknown.

In regards to autophagy, it has recently been reported that autophagic signaling is increased during prolonged MV (18). Nevertheless, the importance of autophagy in VIDD is unknown. While basal autophagy is important for maintaining cell survival by recycling old and damaged organelles and cytosolic proteins; excessive autophagy can induce pathological changes such as apoptosis and muscle atrophy. Therefore, these experiments investigated the role that FOXO and autophagy play in the diaphragm during VIDD. More specifically, these experiments were designed to achieve the following specific aims.

Specific Aim 1: To determine if FOXO-mediated transcription is essential for MV-induced diaphragm weakness. Our work indicates that calpain plays a prominent role in diaphragmatic injury during MV. It is also known that calpain can activate FOXO. In addition, expression of dn FOXO affords protection in other models of disuse muscle atrophy. Therefore, we hypothesize that the expression of a dn FOXO in the diaphragm will attenuate MV-induced diaphragm contractile dysfunction and atrophy.

Specific Aim 2: To establish the role of autophagy in MV-induced diaphragm weakness. Evidence suggests that autophagy is increased in the diaphragm during

MV. However, the relative contribution of autophagy to MV-induced diaphragm contractile dysfunction and atrophy remain unknown. Therefore, we hypothesize that inhibition of autophagy during MV will protect the diaphragm from MV-induced atrophy and weakness.

Specific Aim 3: To determine if decreased FOXO expression will protect against MV-induced expression of autophagy-related genes. It has been shown that FOXO activation is responsible for the transcription of many autophagy genes in locomotor muscles. However, the MV-induced signaling pathways that activate autophagy in the diaphragm remain unknown. Therefore, we hypothesize that expression of a dn FOXO in the diaphragm during MV will result in a decrease in MV-induced expression of autophagy-related genes.

CHAPTER 2
LITERATURE REVIEW

Mechanical ventilation (MV) is used clinically to achieve adequate pulmonary gas exchange in patients that are incapable of maintaining adequate alveolar ventilation on their own. The withdrawal of patients from MV is referred to as “weaning” and although MV is a life-saving intervention, problems in weaning from MV are common. Numerous studies indicate that ventilator-induced diaphragm dysfunction (VIDD), due to both atrophy and contractile dysfunction, is an important contributor in weaning difficulties (39, 40, 50, 52).

Although the specific mechanisms responsible for VIDD remain unknown, it is now clear that increased proteolysis plays a major role in regulating the signaling processes leading to VIDD (26, 29, 51). It follows that understanding the signaling pathways regulating MV-induced protein breakdown is important. Hence, this forms the rationale for the experiments contained within this dissertation. Specifically, our experiments were designed to investigate the role that the ubiquitin/proteasome pathway and the autophagy/lysosomal pathway play in VIDD.

This chapter will discuss the importance of our experimental work and will develop the rationale behind our hypotheses based upon prior research and the work of others. Specifically, this review will be divided into two segments. These segments include: 1) an overview of VIDD; and 2) a detailed discussion of proteolytic pathways in skeletal muscle.

Overview of Ventilator-Induced Diaphragm Dysfunction

Mechanical ventilation (MV) is used clinically for patients with respiratory distress. Specifically, when an individual is unable to sustain adequate alveolar

ventilation on their own, MV is required to maintain adequate gas exchange. Unfortunately, problems in weaning patients from MV are common (~30% of patients) (23). MV-induced diaphragm weakness is clinically important because the most frequent cause of weaning difficulty is respiratory muscle failure due to inspiratory muscle weakness and/or a decline in inspiratory muscle endurance (21, 61). In this regard, the diaphragm is the most important inspiratory muscle.

Importantly, numerous studies indicate that MV-induced diaphragmatic weakness, due to both atrophy and contractile dysfunction, is an important contributor to weaning difficulties (20, 25, 58). Of economic significance is the fact that weaning procedures account for ~40% of the time spent on the ventilator; and this additional hospital time results in additional costs to patients and insurance companies (11). Therefore, improving our understanding of the cellular mechanism(s) responsible for MV-induced diaphragm weakness is necessary for developing a therapeutic intervention to counteract this important and expensive clinical problem.

Diaphragm Response to Mechanical Ventilation

There is abundant evidence from many animal models of MV (rabbits, pigs and baboons) that support the concept that prolonged MV results in VIDD (1, 5, 14, 22, 39, 40, 47). These animal models of MV report a wide array of detrimental effects on the diaphragm. Specifically, rodent studies have observed decreased diaphragm performance during periods lasting from 12-48 hours (6, 39, 50). In this regard, limited human MV studies exist due to the invasive nature of obtaining a biopsy from human diaphragm. However, recent human studies demonstrate that prolonged MV results in diaphragm atrophy. Importantly, these studies by Levine and colleagues report an ~40% decrease in cross-sectional area of both type I and type IIa diaphragm fibers in patients

ventilated between 18-72 hours (25). In addition, in another human study investigators found that twitch transdiaphragmatic pressure generation (i.e. index of diaphragmatic force generation) was 50% lower that healthy patients following MV (58). Finally, a retrospective analysis of postmortem data obtained from neonates who received ventilator assistance for 12 days or more reported diffuse diaphragmatic fiber atrophy, which was not observed in locomotor muscles (20). Collectively these studies clearly document the damaging effects of MV on the human diaphragm.

Mechanisms of MV-induced Diaphragmatic Dysfunction

Diaphragm contractile dysfunction

Problems in weaning patients from MV are often associated with respiratory failure. In this regard, our laboratory has shown that there is a significant decrease in diaphragm specific force production as time on the ventilator is increased. Specifically, maximal diaphragmatic specific force is ~18% lower in animals ventilated for 12 hours and ~46% lower in animals ventilated for 24 hours, when compared to control animals (39). In addition, other groups have shown similar results. For example, Anzueto and collegues have shown decrease in both maximal diaphragmatic force production and endurance after 11 days of MV in baboons and Le Bourdelles et al. have demonstrated a 60% reduction in maximal diaphragm specific force following 48 hours of MV in a rat model (1, 22).

Diaphragm atrophy

MV-induced diaphragm atrophy has been reported in both animal and human experiments (25, 28, 29). A unique characteristic of MV-induced diaphragm atrophy is the rate in which the diaphragm atrophies. While atrophy occurs during all modes of disuse-induced atrophy in skeletal muscles, the rate of MV-induced diaphragm atrophy

is extremely fast. Specifically, whereas it takes a minimum of three days to see significant atrophy of the hindlimb muscles using an immobilization model, there is significant atrophy of the diaphragm muscle fibers in an as few as 12 hours of MV.

Protein synthesis and degradation

MV-induced diaphragm atrophy and contractile dysfunction occur due to both a reduction in diaphragm protein synthesis and an increase in protein degradation. However, work from our lab reveals that MV-induced protease activation is the predominant factor responsible for the rapid onset of diaphragm atrophy during prolonged MV (37, 51, 59). This MV-induced proteolysis in the diaphragm occurs via a highly coordinated interaction between four major proteolytic systems: 1) calpains; 2) caspase-3; 3) ubiquitin-proteasome system; and 4) autophagic/lysosomal system.

Calpain. Calpains are calcium activated proteases that contribute to muscle atrophy by cleaving structural proteins. Studies indicate that calpain cleavage of Z line associated proteins (i.e. titin and nebulin) contributes to the release of myofilament proteins (15). It follows that calpain activation may contribute to skeletal muscle atrophy by releasing myofilaments for subsequent breakdown by the ubiquitin-proteasome system (15). However, recent evidence reveals that calpain may work in conjunction with caspase-3 to degrade actomyosin complexes (10). Indeed, new findings indicate that caspase-3 activation is a required initial step in skeletal muscle catabolism in a variety of wasting conditions including MV-induced diaphragm wasting (10, 38).

In addition to contributing to muscle wasting through the release of myofibrillar proteins, it has also been suggested that calpain activation may be responsible for the activation of FOXO3a which would lead to the transcription of specific atrophy genes (53, 54). Specifically, it has been shown that calpain activation reduces Akt

phosphorylation (53). There is strong evidence that Akt is a negative regulator of FOXO transcription factors and therefore the finding that calpain activation reduces Akt phosphorylation suggest that calpain activation may promote the activation of FOXO transcription factors which could lead to increased muscle proteolysis (53).

Caspase-3. Caspase-3 is a cysteine protease and caspase-3 activation is required for MV-induced atrophy to occur (10). Caspase-3 activation can contribute to MV-induced diaphragmatic atrophy in two important ways. First, active caspase-3 degrades numerous cellular proteins including actomyosin complexes. Second, caspase-3 activation is essential for nuclear apoptosis in the diaphragm during prolonged MV (10, 28). This MV-induced loss of myonuclei in the diaphragm is important because a loss of nuclei diminishes the synthesis of nuclear gene products per unit of diaphragm muscle area and therefore, contributes to reduced protein synthesis and fiber atrophy (10, 28). Hence, caspase-3 activation can contribute to diaphragmatic atrophy by both increasing protein breakdown and decreasing protein synthesis. Finally, caspase-3 may also contribute to proteolytic processing through an interaction with calpain, and MV-induced ROS production can accelerate proteolysis in muscle fibers by oxidizing muscle proteins, which enhances their susceptibility to proteolytic processing by both calpain and caspase-3.

Ubiquitin-Proteasome System. The total proteasome complex (26S proteasome) is comprised of a core proteasome subunit (20S) coupled with two regulatory complexes (19S) located at either end of the 20S core. The 20S proteasome degradation pathway is only active after ubiquitin covalently binds to protein substrates and marks them for degradation. The binding of ubiquitin to protein substrates requires

a three-step process. First, the ubiquitin-activating enzyme (E1) activates ubiquitin. Following activation, the ubiquitination of specific proteins is provided be one of a variety of ubiquitin conjugating enzymes (E2s) and by specialized ubiquitin ligases (E3s) that recognize specific protein substrates. Among these enzymes, E3 ligases are critically important because they account for the substrate specificity in the system. Numerous E3 ligases exist and the muscle specific E3 ligases atrogin-1/MAFbx and MuRF1 have both been reported to be important in muscle protein degradation during disuse atrophy (2, 55).

More specifically, the FOXO family of transcription factors regulates atrogin-1 and MuRF1 expression (46). As previously described, the FOXO class of transcription factors is a downstream target of Akt. Under normal conditions, Akt blocks the function of FOXO which leads to its sequestration in the cytoplasm away from target genes. Dephosphorylation of FOXO factors leads to nuclear entry causing the induction of atrogin-1 and MuRF-1 and increasing muscle atrophy (18, 46).

Autophagic/Lysosomal proteases. Autophagy is a highly regulated lysosomal pathway for the degradation of non-myofibril cytosolic proteins and organelles (4, 45). During autophagy, cytosolic components are sequestered into double membrane vesicles called autophagasomes, which are delivered to lysosomes forming autolysosomes. After docking and fusion with the lysosome, these cytosolic constituents are degraded by lysosomal proteases (i.e. cathepsins) that are the cellular proteases charged with the removal of both organelles and non-myofibril cytosolic protein aggregates.

Our understanding of the molecular mechanisms that regulate autophagy has advanced in recent years. Currently, 31 autophagy-related genes are known in yeast and many homologues of these genes also exist in mammals. These autophagy-related genes and the proteins they express are all described by the common name Atg followed by the number to identify the specific gene or protein (e.g. Atg1, Atg2, etc.). The precise role that each of these 31 Atg proteins play in autophagy continues to be investigated but it appears that at least 18 Atg proteins are involved in the induction of autophagy and autophagosome formation in cells; hence these Atg proteins are required for autophagy to occur. The induction of autophagy occurs by activation of the Atg1 complex which is followed by a cascade of reactions resulting in autophagosome formation. For example, the mammalian homologue of yeast Atg6, beclin-1, associates with numerous autophagy regulatory proteins and is required for induction of autophagy (i.e., formation of the pre-autophagosome structure). Further, the autophagy-related protein Atg7 is also required for the formation and expansion of the autophagosome. The microtubule associated protein light chain, LC3, a mammalian homologue of yeast Atg8, is also essential for expansion of the autophagosome. Finally, numerous lysosomal proteases exist (e.g., cathepsin B, D, H, L) and each plays a vital role in autophagy-related protein breakdown (4, 45).

Although basal autophagy is important for maintaining cell survival by recycling damaged organelles and cytosolic proteins, excessive autophagy can induce pathological changes such as apoptosis, cell death and atrophy. This has been observed in various conditions and is possible related to the fact that there is a simultaneous induction of the autophagic/lysosomal system and the ubiquitin-

proteasome system in the diaphragm during MV (18). A potential mechanism linking these two systems is the increase in oxidative stress that has been recorded in the diaphragm during MV. The induction of the autophagic/lysosomal system and the ubiquitin-proteasome system by oxidative stress may be mediated by FOXO signaling (18). Specifically, activation of FOXO increases the expression of the autophagy genes BNIP3 and LC3. Therefore, FOXO signaling and autophagy may play an important role in skeletal muscle atrophy signaling pathways.

Summary

In conclusion, it has been shown that both the ubiquitin-proteasome and autophagy signaling pathways are important in disuse skeletal muscle atrophy and may be involved in MV-induced diaphragmatic weakness and thus difficulty in “weaning”. In addition, FOXO3a may independently control protein breakdown in skeletal muscle via the ubiquitin-proteasome system and the autophagic/lysosomal system (11). Specifically, markers of autophagy have been shown to be increased during MV as well as specific E3 ligases and therefore FOXO3a and these proteolytic systems may contribute to MV-induced diaphragm weakness. Therefore these experiments investigated the role that FOXO3a and autophagy play in the diaphragm during MV-induced diaphragm atrophy and contractile dysfunction to determine the therapeutic potential for targeting FOXO3a and/or autophagy during MV.

CHAPTER 3
MATERIALS AND METHODS

This chapter will be divided into two sections. The first section will include the experimental design used for each of our experiments, which were intended to determine if FOXO and autophagy signaling contribute to ventilator-induced diaphragm dysfunction (VIDD). In the second section, we will provide the methodological details associated with each experimental protocol and measurement technique.

Experiment 1: Animals

Animal Model Justification

To address our first specific aim and establish whether FOXO expression is required for mechanical ventilation (MV)-induced proteolysis, we used adult female Sprague-Dawley (SD) rats in experiment 1. Animals were 4-6 months old at the time of sacrifice. The SD rat was chosen due to the similarities between the rat and human diaphragm in both anatomical and physiological parameters (2, 3, 31, 32, 35, 36).

Animal Housing and Diet

All animals were housed at the University of Florida Animal Care Services Center according to guidelines set forth by the Institutional Animal Care and Use Committee. The Animal Care and Use Committee of the University of Florida approved these experiments. Animals were maintained on a 12:12 hour light-dark cycle and provided food and water *ad libitum* throughout the experimental period.

Experimental Design

Four experimental groups were used in experiment 1. Animals were randomly assigned to one of the following groups: 1) acutely anesthetized control with GFP (n=8); 2) acutely anesthetized control with dn FOXO (n=8); 3) 12 hours of MV with GFP (n=8);

and 4) 12 hours of MV with dn FOXO (n=8) (Figure 3-1).Group sample size was chosen based on preliminary experiments.

Packaging and Purification of Recombinant AAV Vectors

The DsRed-dnFOXO was a gift of Dr. Andrew Judge (University of Florida, Gainesville) and has been previously described (42). We constructed the pTRUF12-DsRed-dnFOXO plasmid by PCR amplifying the DsRed-dnFOXO sequence into the SpeI and ClaI sites of pTRUF12. Verification of the appropriate fusion sequence was performed by DNA sequencing at the University of Florida DNA Sequencing Core Facility. The EGFP expressing empty vector, pTRUF12 was used as a control plasmid. The rAAV pTRUF12-DsRed-dnFOXO and pTRUF12 were generated, purified and tittered at the University of Florida Gene Therapy Center Vector Core Lab as previously described (62).

Animal Protocol

All animals in this experiment underwent a survival surgery 4 weeks prior to MV. For the survival surgery animals were anesthetized to a surgical plane of anesthesia with isoflurane. Animals were initially anesthetized using 2-4% inhaled isoflurane followed with continuous anesthesia with 0.5-2.5% inhaled isoflurane administered through the surgical procedure. After reaching a surgical plane of anesthesia a midline abdominal incision was made extending from the xyphoid process to the suprapubic region to expose the surface of the diaphragm. Eight evenly spaced intramuscular injections were made along the diaphragm with either the pTRUF12 or pTRUF12-DsRed-dnFOXO. Following this procedure the abdominal muscles and the skin were sutured and closed and the animals received 1cc 0.9% Sodium Chloride and

Buprenorphine (0.05-0.1 mg/kg) every 8-12 hours for the first 48 hours after surgery as needed.

After a four week incubation period animals in the control groups were acutely anesthetized with sodium pentobarbital (60 mg/kg IP). After reaching a surgical plane of anesthesia, the control animals were sacrificed immediately. A section of the costal diaphragm was used for contractile measurements while the rest was stored at -80°C for subsequent analysis.

Animals in the MV group were acutely anesthetized with sodium pentobarbital (60 mg/kg IP). After reaching a surgical plane of anesthesia, the animals were tracheostomized utilizing aseptic techniques and mechanically ventilated with a controlled pressure-driven ventilator (Siemens) for 12 hours with the following settings: upper airway pressure limit: 20 cmH_2O, PEEP: 1 cmH_2O, pressure control level above PEEP: 4-6 cm H_2O, and respiratory rate: 80 bpm (6, 57). We chose 12 hours of MV because this time period is associated with diaphragmatic oxidative stress, proteolysis, contractile dysfunction and myofiber atrophy. Surgical preparations, procedures and animal monitoring was performed as previously described (13). Following the completion of each experimental protocol, the animals were immediately sacrificed and a section of the costal diaphragm was used for contractile measurements while the rest was stored at -80°C for subsequent analyses.

Statistical Analysis

Group sample size was determined using a power analysis of preliminary data from our laboratory. Comparisons between groups were made by one-way ANOVA and when appropriate, a Tukey HSD test was performed. Significance was established at $P<0.05$.

Experiment 2: Animals

Animal Model Justification

To address our second specific aim and to determine whether increased autophagy is essential for VIDD, adult female SD rats were used for experiment 2. The animals were 4-6 months of age at the time of sacrifice. The rationale for selecting the rat as an experimental model was discussed previously.

Animal Housing and Diet

All animals were housed at the University of Florida Animal Care Services Center according to guidelines set forth by the Institutional Animal Care and Use Committee. The Animal Care and Use Committee of the University of Florida has approved these experiments. Animals were maintained on a 12:12 hour light-dark cycle and provided food and water *ad libitum* throughout the experimental period.

Experimental Design

Four groups were used in experiment 2. Animals were randomly assigned to one of the following groups: 1) acutely anesthetized control with GFP (n=8); 2) acutely anesthetized control with dn ATG5 (n=8); 3) 12 hours of MV with GFP (n=8); and 4) 12 hours of MV with dn ATG5 (n=8) (Figure 3-2). Group sample size was chosen based on preliminary experiments

Packaging and Purification of Recombinant AAV Vectors

The dn ATG5 plasmid was purchased from addgene. We constructed the pTRUF12-dnATG5 plasmid by PCR amplifying the dnATG5 sequence into the SpeI and ClaI sites of pTRUF12. Verification of the appropriate fusion sequence was performed by DNA sequencing at the University of Florida DNA Sequencing Core Facility. The EGFP expressing empty vector, pTRUF12 was used as a control plasmid. The rAAV

pTRUF12-dnATG5 and pTRUF12 were generated, purified and tittered at the University of Florida Gene Therapy Center Vector Core Lab as previously described (62).

Animal Protocol

All animals in this experiment underwent a survival surgery 4 weeks prior to MV. For the survival surgery animals were anesthetized to a surgical plane of anesthesia with isoflurane. Animals were initially anesthetized using 2-4% inhaled isoflurane followed with continuous anesthesia with 0.5-2.5% inhaled isoflurane administered through the surgical procedure. After reaching a surgical plane of anesthesia a midline abdominal incision was made extending from the xypoid process to the suprapubic region to expose the surface of the diaphragm. Eight evenly spaced intramuscular injections were made along the diaphragm with either a control GFP plasmid or the dn ATG5 plasmid. Following this procedure the abdominal muscles and the skin were sutured and closed and the animals received 1cc 0.9% Sodium Chloride and Buprenorphine (0.05-0.1 mg/kg) every 8-12 hours for the first 48 hours after surgery as needed.

After a four week incubation period animals in the control groups were acutely anesthetized with sodium pentobarbital (60 mg/kg IP). After reaching a surgical plane of anesthesia, the control animals were sacrificed immediately and a section of the costal diaphragm was used for contractile measurements while the rest was stored at -80°C for subsequent analysis.

Animals in the MV group were acutely anesthetized with sodium pentobarbital (60 mg/kg IP). After reaching a surgical plane of anesthesia, the animals were tracheostomized utilizing aseptic techniques and mechanically ventilated with a controlled pressure-driven ventilator (Siemens) for 12 hours with the following settings:

upper airway pressure limit: 20 cmH_2O, PEEP: 1 cmH_2O, pressure control level above PEEP: 4-6 cm H_2O, and respiratory rate: 80 bpm (6, 57). We chose 12 hours of MV because this time period is associated with diaphragmatic oxidative stress, proteolysis, contractile dysfunction and myofiber atrophy. Surgical preparation, procedures and animal monitoring was performed as previously described (13). Following the completion of each experimental protocol, the animals were immediately sacrificed and a section of the costal diaphragm was used for contractile measurements while the rest was stored at -80°C for subsequent analyses.

Statistical Analysis

Group sample size was determined using a power analysis of preliminary data from our laboratory. Comparisons between groups were made by one-way ANOVA and when appropriate, a Tukey HSD test was performed. Significance was established at $P<0.05$.

Experiment 3: Animals

Animal Model Justification

To address our third specific aim and establish whether FOXO expression is required for MV-induced autophagy, we used adult female SD rats in experiment 3. Animals were 4-6 months old at the time of sacrifice. The rationale for selecting the rat as an experimental model was discussed previously.

Animal Housing and Diet

All animals were housed at the University of Florida Animal Care Services Center according to guidelines set forth by the Institutional Animal Care and Use Committee. The Animal Care and Use Committee of the University of Florida has approved these

experiments. Animals were maintained on a 12:12 hour light-dark cycle and provided food and water *ad libitum* throughout the experimental period.

Experimental Design

Four experimental groups were used in experiment 3. Animals were randomly assigned to one of the following groups: 1) acutely anesthetized control with GFP (n=8); 2) acutely anesthetized control with dn FOXO (n=8); 3) 12 hours of MV with GFP (n=8); and 4) 12 hours of MV with dn FOXO (n=8) (Figure 3-1). Group sample size was chosen based on preliminary data.

Packaging and Purification of Recombinant AAV Vectors

The DsRed-dnFOXO was a gift of Dr. Andrew Judge (University of Florida, Gainesville) and has been previously described (42). We constructed the pTRUF12-DsRed-dnFOXO plasmid by PCR amplifying the DsRed-dnFOXO sequence into the SpeI and ClaI sites of pTRUF12. Verification of the appropriate fusion sequence was performed by DNA sequencing at the University of Florida DNA Sequencing Core Facility. The EGFP expressing empty vector, pTRUF12 was used as a control plasmid. The rAAV pTRUF12-DsRed-dnFOXO and pTRUF12 were generated, purified and tittered at the University of Florida Gene Therapy Center Vector Core Lab as previously described (62).

Animal Protocol

All animals in this experiment underwent a survival surgery 4 weeks prior to MV. For the survival surgery animals were anesthetized to a surgical plane of anesthesia with isoflurane. Animals were initially anesthetized using 2-4% inhaled isoflurane followed with continuous anesthesia with 0.5-2.5% inhaled isoflurane administered through the surgical procedure. After reaching a surgical plane of anesthesia a midline

abdominal incision was made extending from the xypoid process to the suprapubic region to expose the surface of the diaphragm. Eight evenly spaced intramuscular injections were made along the diaphragm with either a control GFP plasmid or the dnFOXO plasmid. Following this procedure the abdominal muscles and the skin were sutured and closed and the animals received 1cc 0.9% Sodium Chloride and Buprenorphine (0.05-0.1 mg/kg) every 8-12 hours for the first 48 hours after surgery as needed.

Following a four week incubation period animals in the control groups were acutely anesthetized with sodium pentobarbital (60 mg/kg IP). After reaching a surgical plane of anesthesia, the control animals were sacrificed immediately. A section of the costal diaphragm was used for contractile measurements while the rest was stored at -80°C for subsequent analysis.

Animals in the MV group were acutely anesthetized with sodium pentobarbital (60 mg/kg IP). After reaching a surgical plane of anesthesia, the animals were tracheostomized utilizing aseptic techniques and mechanically ventilated with a controlled pressure-driven ventilator (Siemens) for 12 hours with the following settings: upper airway pressure limit: 20 cmH_2O, PEEP: 1 cmH_2O, pressure control level above PEEP: 4-6 cm H_2O, and respiratory rate: 80 bpm (6, 57). We chose 12 hours of MV because this time period is associated with diaphragmatic oxidative stress, proteolysis, contractile dysfunction and myofiber atrophy. Surgical preparations, procedures and animal monitoring was performed as previously described (13). Following the completion of each experimental protocol, the animals were immediately sacrificed and

a section of the costal diaphragm was used for contractile measurements while the rest was stored at -80°C for subsequent analyses.

Statistical Analysis

Group sample size was determined using a power analysis of preliminary data from our laboratory. Comparisons between groups were made by one-way ANOVA and when appropriate, a Tukey HSD test was performed. Significance was established at $P<0.05$.

General Methods

Histological Measures

Myofiber Cross-Sectional Area. Diaphragms were removed and fixed in OCT and stored at -80°C. On the day of analysis, sections from frozen diaphragm samples were cut at 10 microns with a cryotome (Shandon Inc., Pittsburg, PA) and allowed to air dry at room temperature for 30 minutes. Sections were stained for dystrophin, myosin heavy chain (MHC) I and MCH type IIa proteins for fiber cross-sectional area (CSA) as previously described (28). CSA was determined using Scion software (NIH).

LC3 Immunohistochemistry. Sections from frozen diaphragm samples were cut at 10 microns using a cryotome and fixed in 4% paraformaldehyde for 20 minutes. Sections were then washed in PBS and blocked with 5% bovine serum albumin (BSA) and 3% goat serum in PBS. LC3 primary (Cell Signaling Technology) and secondary (alexa Fluro 488 goat anti-rabbit) reagents were diluted in 1% BSA. Sections were mounted with fluorescent mounting medium with Dapi (Vector Laboratories) and images were acquired via a monochrome camera (Qimaging Retiga) attached to an inverted fluorescent microscope (Axiovert 200, Xeiss).

Functional Measures

Contractile Properties. Upon sacrifice or the completion of the mechanical ventilation period, the entire diaphragm was removed and placed in a dissecting chamber containing a Krebs-Hensleit solution equilibrated with 95% O_2-5% CO_2 gas. A muscle strip, including the tendinous attachments at the central tendon and rib cage was dissected from the midcostal region. The strip was suspended vertically between two lightweight Plexiglas clamps with one end connected to an isometric force transducer (model FT-03, Grass Instruments, Quincy, MA) within a jacketed tissue bath. The force output was recorded via a computerized data-acquisition system (Super Scope II, GW Instruments Somerville, MA; Apple Computer Cupertino, CA). The tissue bath was filled with Krebs-Hensleit saline and the buffer was aerated with gas (95% O_2-5% CO2), pH was maintained at 7.4, and the osmolality of the bath was ~290 mosmol/kgH_2O. After a 15-min equilibration period (25°C), *in vitro* diaphragmatic contractile measurements were made. The muscle strip was stimulated along its entire length with platinum wire electrodes (modified S48 stimulator, Grass Instruments) by using supramaximal (~150%) stimulation voltage to determine the optimum contractile length (*L*o). *L*o was determined by systematically adjusting the length of the muscle using a micrometer while evoking single twitches. Thereafter, all contractile properties were measured isometrically at *L*o. To measure maximal isometric twitch force each strip was stimulated supramaximally with 120-V pulses at 1 Hz and to measure the force frequency response each strip was stimulated supramaximally with 120-V pulses at 15–160 Hz. The duration of each train was 500 ms to achieve a force plateau. Contractions were separated by a 2-min recovery period. For comparative purposes, diaphragmatic (bundles of fibers) force production was normalized as specific Po. The

total muscle cross-sectional area at right angles to the long axis was calculated by the following algorithm (48): Total muscle cross-sectional area (mm^2) = [muscle mass/(fiber length x 1.056)], where 1.056 is the density of muscle (in g/cm^3). Fiber length was expressed in centimeters measured at *L*o (43).

Biochemical Measures

Western Blot Analysis. Protein abundance was determined in whole diaphragm samples via western blot analysis. Briefly, diaphragm tissue samples were homogenized 1:10 (wt/vol) in 5mM Tris (pH 7.5) and 5 mM EDTA (pH 8.0) with a protease inhibitor cocktail (Sigma, St. Louis, MO) and centrifuged at 1,500 g for 10 min at 4°C. After the resulting supernatant was collected, diaphragm protein content was assessed by the method of Bradford (Sigma). Proteins from the supernatant fraction were separated via polyacrylamide gel electrophoresis via 4-20% gradient polyacrylamide gels containing 0.1% SDS for ~1 h at 200 V. After electrophoresis, the proteins were transferred to nitrocellulose membranes and incubated with primary antibodies directed against proteins of interest. Following incubation with primary antibodies, membranes were washed extensively with PBS-Tween and then incubated with secondary antibodies (GE Healthcare, Piscataway, NJ). After being washed, a chemiluminescent system was used to detect labeled proteins (GE Healthcare). Membranes were developed using autoradiography film and images of the film were captured and analyzed using the 440CF Kodak Imaging System (Kodak, New Haven, CT).

RNA Isolation and cDNA Synthesis. Total RNA was isolated from muscle tissue with TRIzol Reagent (Life Technologies, Carlsbad, CA) according to the manufacturer's instructions. RNA content (μg/mg muscle) was evaluated by spectrophotometry and

RNA (5µg) was then reverse transcribed with the Superscript III First-Strand Synthesis System for RT-PCR (life Technologies), using oligo(dT)20 primers and the protocol outlined by the manufacturer.

Real-time Polymerase Chain Reaction. One microliter of cDNA was added to a 25 µl PCR reaction for real-time PCR using Taqman chemistry and the ABI Prism 7000 Sequence Detection system (ABI, Foster City, CA). Relative quantification of gene expression was performed using the comparative computed tomography method (ABI, User Bulletin no. 2). This method uses a single sample, the calibrator sample (*β-glucuronidase*;GenBank NM Y00717, NM M13962), for comparison of every unknown sample's gene expression. ΔΔCT[ΔCT(calibrator)−ΔCT(sample)] was then calculated for each sample and relative quantification was calculated as 2ΔΔCT. *β-Glucuronidase*, a lysosomal glycoside hydrolase, was chosen as a reference gene based on previous work showing unchanged expression with our experimental manipulations (8, 9). Fivefold dilution curves were assayed on selected samples to confirm the validity of this quantification method for each gene. MAFbx, MuRF-1, FOXO3, BNIP3, LC3, Beclin, ATG12, ATG5, ATG7, Cathepsin B, Cathepsin D and Cathepsin L mRNA transcripts were assayed using predesigned rat primer and probe sequences commercially available from Applied Biosystems (Assays-on-Demand).

Electron Microscopy. Diaphragm samples were cut into $1mm^2$ sections. Sections were fixed in 4% paraformaldehyde and 2.5% glutaraldehyde (pH 7.25). Samples were analyzed by the University of Florida ICBR Electron Microscopy Core Lab.

Mitochondrial Measures

Preparation of Permeabilized Muscle Fibers. Approximately 25 mg of costal diaphragm muscle were dissected and placed on a plastic Petri dish containing ice-cold

buffer X (60 mM K-MES, 35 mM KCl, 7.23 mM K_2EGTA, 2.77 mM CaK_2EGTA, 20 mM imidazole, 0.5 mM DTT, 20 mM taurine, 5.7 mM ATP, 15 mM PCr, and 6.56 mM $MgCl_2$, pH 7.1). The muscle was trimmed of connective tissue and cut down to fiber bundles (4-8 mg wet wt). The muscle fiber bundles were gently separated in ice-cold buffer X to maximize surface area of the fiber bundle. To permeabilize the myofibers, each fiber bundle was incubated in ice-cold buffer X containing 50µg/ml saponin on a rotator for 30 min at 4°C. The permeabilized muscle bundles were then washed in ice-cold buffer Z (110 mM K-MES, 35 mM KCl, 1 mM EGTA, 5 mM K_2HPO4, and 3 mM $MgCl_2$, 0.005 mM glutamate, and 0.02 mM malate and 0.5 mg/ml BSA, pH 7.1).

Mitochondrial Respiration. Respiration was measured polarographically in a respiration chamber maintained at 37°C (Hanstech Instrumnets, United Kingdom). After the respiration chamber was calibrated, permeabilized fiber bundles were incubated with 1 ml of respiration buffer Z containing 20mM creatine to saturate creatine kinase. Flux through complex I was measured using 5mM pyruvate and 5mM malate. The ADP-stimulated respiration (state 3) was initiated by adding 0.25 mM ADP to the respiration chamber. Basal respiration (state 4) was determined in the presence of 10 µg/ml oligomycin to inhibit ATP synthesis. The respiratory control ration (RCR) was calculated by dividing the state 3 by state 4 respiration.

Mitochondrial ROS Emission. Diaphragmatic mitochondrial ROS emission was determined using Amplex Red (Molecular Probes, Eugene, OR). Details of this assay have been described previously (19). Mitochondrial ROS production was measured using the creatine kinase energy clamp technique to maintain respiration at steady state using previously described methods (30).

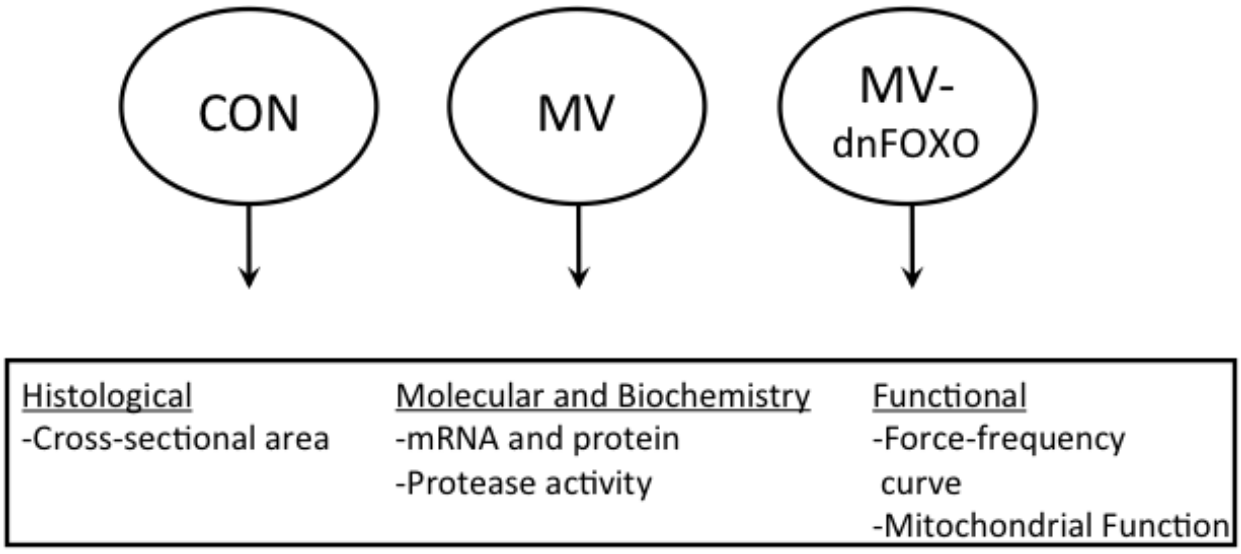

Figure 3-1. Experimental animal design used to determine the effect of blocking FOXO transcription during MV on diaphragm function and activation of proteolytic pathways. This experimental design was used for Specific Aim 2.

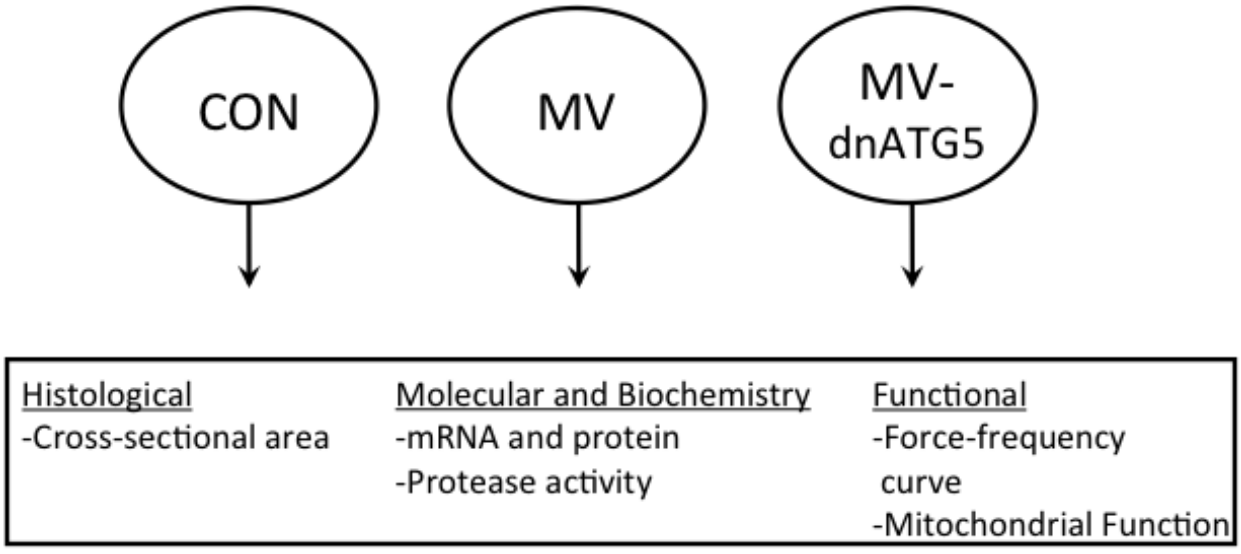

Figure 3-2. Experimental animal design used to determine the effect of blocking Atg5 activation during MV on diaphragm function and activation of proteolytic pathways. This experimental design was used for Specific Aim 2.

CHAPTER 4
RESULTS

Experiment 1: Systemic Response to Mechanical Ventilation

Experiment 1 was designed to determine if FOXO-mediated transcription is essential for mechanical ventilation (MV)-induced diaphragm weakness. Animals used in this experiment were 4-6 months of age and prior to the initiation of MV no significant differences existed in body weight between groups (CON = 296g ± 4, CON-dnFOXO = 299g ± 7, MV = 301g ± 6, MV-dnFOXO = 302g ± 6). Importantly, 12 hours of MV did not significantly alter the body weight of the MV or MV-dnFOXO group ($P<0.05$). Our results also indicate that during MV, systolic blood pressure (MV = 104 ± 7, MV-dnFOXO = 109 ± 3 mmHg), heart rate (MV = 356 ± 7, MV-dnFOXO = 366 ± 7), PaO_2 (MV = 81 ± 2, MV-dnFOXO = 82 ± 3 mmHg), $PaCO_2$ (MV = 37 ± 2, MV-dnFOXO = 35 ± 2 mmHg) and pH (MV = 7.45 ± 0.01, MV-dnFOXO = 7.45 ± 0.01) did not significantly differ between the ventilated groups. Furthermore, at the completion of 12 hours of MV, there were no visual abnormalities of the lungs or peritoneal cavity and no evidence of infection, indicating that our aseptic surgical technique was successful.

Redox Balance

4-HNE

Previous work from our laboratory demonstrates that MV-induced oxidative stress in the diaphragm is a required upstream trigger that is responsible for signaling events leading to ventilator-induced diaphragm dysfunction (VIDD) (6, 13, 29). In this regard, lipid peroxidation occurs in the diaphragm due an imbalance in oxidant production/removal resulting in the production of biologically active aldehydes. 4-hydroxynoneal (4-HNE) is an unsaturated α,β hydroxyalkenal that is generated during

the lipid peroxidation cascade. Compared to control (CON), MV resulted in a significant increase in 4-HNE protein adducts in the diaphragm. MV combined with dnFOXO (MV-dnFOXO) did not attenuate the increase in 4-HNE modified protein accumulation ($P<0.05$) (Figure 4-1).

Mitochondrial Reactive Oxygen Species Emission

Mitochondria have been shown to be the primary source of reactive oxygen species (ROS) in the diaphragm during MV. Inhibition of MV-induced mitochondrial ROS production is sufficient to protect the diaphragm against VIDD (37). The current data shows that diaphragm mitochondrial H_2O_2 release is increased during MV and treatment of animals with dnFOXO did not protect against MV-induced increases in diaphragm mitochondrial ROS production during both state 3 and state 4 respiration ($P<0.05$) (Figure 4-2).

Diaphragm Function

Mitochondrial Function

Respiratory control ratio. As previously described, mitochondria are the most important source of ROS in the diaphragm during MV (19, 37). In this regard, compared to CON, our data indicate that MV results in a significant decrease in diaphragmatic mitochondrial coupling as evidence by a decrease in the RCR ($P<0.05$). In addition, mitochondrial respiratory control ratio (RCR) in the MV-dnFOXO group was also significantly reduced compared to CON ($P<0.05$) (Table 4-1).

Contractile Function

Force-frequency response. The diaphragm force-frequency response was measured in our experimental groups to determine the effectiveness of dnFOXO administration in maintaining diaphragm contractile function during MV. The mean

specific force-frequency responses from CON, CON-dnFOXO, MV and MV-dnFOXO treated animals are shown in Figure 4-3. Twelve hours of MV resulted in a significant reduction ($P<0.05$) in the specific force of the diaphragm compared to the CON group at all stimulation frequencies. Additionally, compared to CON, treatment of non-ventilated animals with dnFOXO did not result in any change to the force production of the diaphragm at any stimulation frequency. Finally, treatment of mechanically ventilated animals with dnFOXO prior to MV did not provide protection against MV-induced decreases in diaphragm force production.

Diaphragm Structure

Cross-sectional area. To evaluate the impact of FOXO signaling on prolonged MV-induced diaphragm atrophy we measured the cross-sectional area (CSA) of diaphragm muscle fibers across our experimental groups. Compared to CON we observed a significant ($P<0.05$) decrease in diaphragm Type I, Type IIa and Type IIx/b fiber CSA following MV (Figure 4-4). In addition, there was no difference in CSA in CON animals, compared to CON-dnFOXO animals, which confirms that FOXO signaling alone is not responsible for MV-induced diaphragm atrophy. Finally, treatment with dnFOXO resulted in protection against MV-induced atrophy of all diaphragmatic fiber types.

Proteolytic Activity

Calpain

Calpain is a calcium-activated protease that is required for VIDD. In this regard, it is possible that calpain signaling acts as an upstream trigger to signal the activation of FOXO activity (53). Calpain activity in the diaphragm was evaluated by western blotting techniques to determine both the active band of calpain 1 as well as the calpain-

specific spectrin breakdown product (SBDP) (Figure 4-5). Our results show that calpain activity is increased in the diaphragm during MV, and expression of dnFOXO did not prevent the increase in diaphragmatic calpain activity during MV ($P<0.05$).

Caspase-3

Caspase-3 is a protease that is capable of degrading intact actomyosin proteins and it also plays a key role in promoting myonuclear apoptosis in muscle fibers. Compared to control animals, MV resulted in a significant increase in both cleaved (active) caspase-3 and an increase in the protein levels of the caspase-3 specific SBDP in the diaphragm ($P<0.05$) (Figure 4-6). Inhibition of FOXO prior to MV resulted in no significant reduction of active caspase-3 in the diaphragm compared to non-treated MV animals.

Ubiquitin-Proteasome System

FOXO signaling has been shown to be required for activation of the proteasome system of proteolysis. Specifically, active FOXO is responsible for the increased transcription of the muscle specific E3 ligases Atrogin-1 and MuRF1. Our results demonstrate that MV results in an increase in the mRNA and protein expression of both Atrogin-1 (Figure 4-7) and MuRF1 in the diaphragm (Figure 4-8). However, prevention of FOXO signaling in the diaphragm by treatment with the dnFOXO prevented the MV-induced increase in atrogin-1 and MuRF1 mRNA and protein abundance in the diaphragm. This indicates that our gene transfection was successful and that treatment with dnFOXO prior to MV can prevent the MV-induced increase in FOXO signaling in the diaphragm.

Experiment 2: Systemic Response to MV

Experiment 2 investigated the role that autophagy plays in MV-induced diaphragm weakness. Animals used in this experiment were 4-6 months of age and prior to the initiation of MV no significant differences existed in body weigh between groups (CON = 298g ± 4, CON-dnATG5 = 296g ± 4, MV = 301g ± 6, MV-dnATG5 = 301g ± 7). Importantly, 12 hours of MV did not significantly alter the body weight of the MV or MV-dnATG5 group ($P<0.05$). Our results also indicate that during MV, systolic blood pressure (MV = 105 ± 5, MV-dnATG5 = 106 ± 3 mmHg), heart rate (MV = 356 ± 7, MV-dnATG5 = 367 ± 6), PaO_2 (MV = 81 ± 2, MV-dnATG5 = 82 ± 3 mmHg), $PaCO_2$ (MV = 37 ± 2, MV-dnATG5 = 34 ± 2 mmHg) and pH (MV = 7.45 ± 0.01, MV-dnATG5 = 7.46 ± 0.01) were not significantly different between the ventilated groups. Furthermore, at the completion of 12 hours of MV, there were no visual abnormalities of the lungs or peritoneal cavity and no evidence of infection, indicating that our aseptic surgical technique was successful.

Redox Balance

4-HNE

As previously described, the induction of oxidative stress is a required upstream trigger that is responsible for signaling events leading to VIDD (6, 29, 37). 4-HNE is the primary adduct formed during lipid peroxidation and is commonly used to assess protein damage. Compared to CON, both MV groups demonstrated a significant increase in 4-HNE protein content ($P<0.05$) (Figure 4-9).

Mitochondrial ROS

The mitochondria have been shown to be a major source of ROS in the diaphragm during MV, and our results confirm this observation. Specifically, compared to CON, MV

resulted in a significant increase in diaphragm mitochondrial H_2O_2 emission during state 4 respiration ($P<0.05$). Interestingly, compared to MV, increased expression of the dnATG5 resulted in a complete attenuation of this MV-induced increase in diaphragm mitochondrial ROS production (Figure 4-10).

Diaphragm Function

Mitochondrial Function

Respiratory control ratio. Our data indicate that 12 hours of MV results in a significant reduction of the RCR in mitochondria within permeabilized diaphragm muscle fiber bundles ($P<0.05$). Specifically, this RCR decline is due to a significant increase in state 4 respiration in MV animals. Importantly, RCR measurements made in the MV-dnATG group reveal that these animals showed a significant attenuation of the MV-induced decrease in RCR (Table 4-2).

Contractile Function

Force-frequency response. To determine the role of autophagy in MV-induced diaphragm force deficits, we measured both the *in vitro* maximal isometric twitch force and force-frequency responses of strips of diaphragm muscle. Compared to CON, MV resulted in a significant reduction in diaphragm muscle force production at all stimulation frequencies tested ($P<0.05$). In addition, to this the MV-dnATG5 animals also produced significantly reduced forces compared to CON (Figure 4-11). In contrast, treatment of control animals with dnATG5 had no effect on diaphragm force production at any stimulation frequency.

Diaphragm Structure

Cross-sectional Area

Myofiber CSA was determined for individual fiber types in diaphragm muscle strips from all experimental groups. Treatment of control animals with dnATG5 resulted in no significant differences in diaphragm fiber CSA compared to CON animals ($P<0.05$). Additionally, compared to CON, prolonged MV resulted in significant atrophy of type I, type IIa and type IIx/b diaphragm myofibers. Further, prolonged MV resulted in significant atrophy of type I, type IIa and type IIx/b diaphragm myofibers compared to both CON and MV-ATG5 animals, indicating that inhibition of ATG5 is capable of attenuating MV-induced diaphragmatic atrophy (Figure 4-12).

Electron Microscopy

To evaluate changes to the diaphragm structure we used electron microscopy to visualize abnormalities caused as a result of prolonged MV as well as to determine if treatment with dnATG5 prior to MV resulted in a decrease in autophagosome formation. Representative diaphragm images from all experimental groups are presented in Figure 4-13. Treatment with dnATG5 appears to decrease autophagosome formation.

Proteolytic Activity

Calpain

Calpain has been shown to be an important protease in muscle wasting and activation of calpain contributes to VIDD. Our results show that MV results in a significant increase in calpain activity in the diaphragm ($P<0.05$). In contrast, inhibiting autophagy (e.g., dnATG5) prior to MV attenuates MV-induced calpain activation in the diaphragm (Figure 4-14).

Caspase-3

Caspase-3 has been shown to degrade myofibrillar proteins and play an important role in VIDD (28). Compared to control animals, MV results in a significant increase in both cleaved (active) caspase-3 and increased protein levels of the caspase-3 specific SBDP in the diaphragm ($P<0.05$) (Figure 4-15). Although our results are not definitive, inhibiting autophagy appears to attenuate the MV-induced activation of caspase-3 in the diaphragm.

Autophagy/Lysosomal System

The autophagy/lysosomal system is comprised of a system of proteins that work together to degrade damaged cytosolic proteins and organelles. In this regard, we measured the mRNA and protein expression of many of these proteins to determine the contribution of autophagy to VIDD. Beclin-1 is a protein that is required for the initiation of autophagosome formation. We found that both the mRNA and protein levels of Beclin 1 are increased in the diaphragm during prolonged MV in both the MV and the MV-ATG5 groups ($P<0.05$)(Figure 4-16). Atg5, Atg12 and LC3 proteins all contribute to the formation of the autophagosome. Specifically, Atg5 and Atg12 form a complex that aids in the elongation of the autophagosome. Our data reveals that MV results in a significant increase in the diaphragmatic mRNA levels of both Atg12 and Atg5 ($P<0.05$). However, prolonged MV with dnATG5 treatment did not result in increased diaphragmatic levels of Atg5 and Atg12 mRNA (Figure 4-17). In addition, our findings reveal an increase in the protein concentration of the Atg12-Atg5 complex in the diaphragm during MV ($P<0.05$). However, this response was attenuated in the MV-dnATG5 group (Figure 4-18). Finally, LC3 also contributes to the elongation of the autophagosome and accumulation of LC3II serves as an indicator of increased

autophagic flux. Our data reveal that MV increases LC3 mRNA levels and also raises the ratio of LC3II to LC3I in the diaphragm. Importantly, these MV-induced increases are attenuated in animals treated with the dnATG5 ($P<0.05$) (Figure 4-19). Finally, as a second marker of LC3 accumulation we stained diaphragm muscle cross-sections with an LC3 antibody. These results indicate that compared to CON, prolonged MV results in a significant increase in LC3 within diaphragm muscle fibers. Expression of the dnATG5 in the diaphragm was sufficient to decrease MV-induced LC3 accumulation in the diaphragm (Figure 4-20).

Experiment 3: Systemic Response to MV

Experiment 3 determined if decreased FOXO expression will protect against MV-induced expression of autophagy-related genes in the diaphragm. Animals used in this experiment were the same animals used in experiment 1. No visual abnormalities appeared in any experimental group after MV.

Diaphragm Structure

Electron Microscopy. To evaluate changes to the diaphragm structure we used electron microscopy to visualize abnormalities caused as a result of prolonged MV. In addition, we determined if treatment with dnFOXO prior to MV resulted in a decrease in autophagosome formation. Representative images of diaphragm muscle from all experimental groups appear in Figure 4-21.

Autophagic/Lysosomal System

Autophagosome Initiation

Beclin 1 is an autophagy gene that plays an important role during the initial steps of autophagosome formation. Therefore, Beclin 1 can be measured as an indicator of autophagy initiation. Our results reveal that MV caused a significant increase in both the

mRNA and protein expression of Beclin 1 in the diaphragm which inhibition of FOXO signaling did not attenuate (P<0.05) (Figure 4-22).

Autophagosome Formation

Autophagosome formation requires the coordination of many different autophagy genes. Specifically, Atg4, Atg7 and LC3 are all involved in the formation of the autophagosome. Our results reveal that there is a significant increase in Atg4 mRNA and protein levels in the diaphragm of MV animals compared to CON animals(P<0.05). Notably, prevention of FOXO signaling attenuated the MV-induced increase in Atg4 expression in the diaphragm (Figure 4-23). Atg7 mRNA and protein levels were also increased in the diaphragm following prolonged MV (P<0.05). Similarly to Atg4, prevention of signaling (i.e., dnFOXO) prevented the MV-induced increase in Atg7 expression in the diaphragm (Figure 4-24). Finally, LC3 is a transcriptional target of FOXO activity and LC3 is a key protein in autophagosome formation. During autophagy, the cytoplasmic form of LC3 is recruited to the autophagosome where LC3 II is generated by both proteolysis and lipidation. It follows that the ratio of LC3 II to LC3 I is an excellent biomarker of autophagic activity. Our results show that there is an increase in the ratio of LC3 II to LC3 I in the diaphragm following MV (P<0.05) (Figure 4-25). In addition, there is also an increase of the mRNA expression of LC3 in the diaphragm following MV (P<0.05) (Figure 4-25). Expression of dnFOXO in the diaphragm prevented the MV-induced increase in LC3 mRNA levels in the diaphragm and also prevented the increase in the LC3 II to LC3 I ratio. To further document the impact of FOXO signaling on LC3 accumulation in the diaphragm we stained diaphragm cross-sections to visualize LC3 content in fibers. Prolonged MV resulted in the accumulation

of LC3 in diaphragm muscle fibers, whereas overexpression of dnFOXO during MV prevented this MV-induced increase in LC3 in the diaphragm (Figure 4-26).

Lysosomal Proteases

It is established that several lysosomal proteases participate in autophagy and are activated in skeletal muscle undergoing disuse muscle atrophy (4). Therefore, we measured the mRNA levels and protein abundance of the lysosomal protease cathepsin L (Figure 4-27). Our data reveals that the mRNA expression of cathepsin L is increased in the diaphragm following prolonged MV. In addition, there is also a significant increase in cathepsin L protein abundance in the diaphragm following MV. Importantly, inhibition of FOXO signaling prevented the MV-induced increase in cathepsin L protein levels and significantly attenuated the increase cathepsin L mRNA in the diaphragm ($P<0.05$).

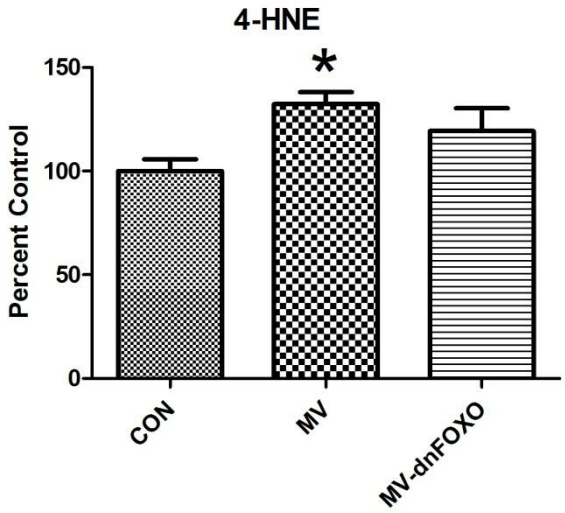

Figure 4-1. The levels of 4 hydroxynonenal (4-HNE) were analyzed as an indicator of lipid peroxidation via western blotting for experiment 1. Values are mean percentage change ± SE and normalized to α-tubulin. * Significantly different versus CON (P<0.05).

A) B)

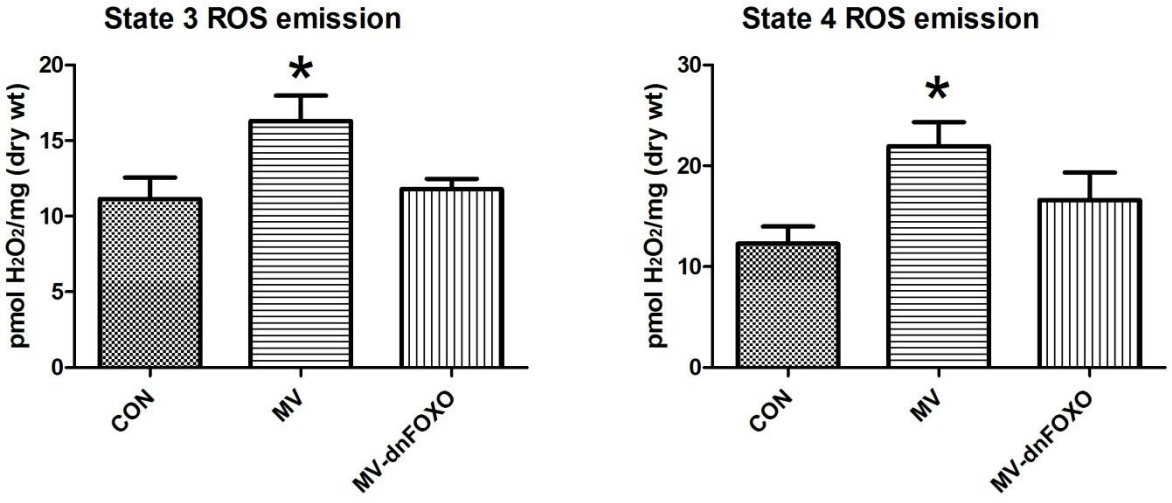

Figure 4-2. Rates of hydrogen peroxide release (H_2O_2) release from permeabilized diaphragm muscle fibers for experiment 1. Values are mean ± SE. A) State 3 ROS emission B) State 4 ROS emission. * Significantly different versus CON (P<0.05).

Table 4-1. Mitochondrial respiratory function in permeabilized fibers from diaphragm muscle obtained from non-mechanically ventilated (CON), mechanically ventilated animals (MV) and mechanically ventilated animals with dnFOXO administration (MV-dnFOXO).

	CON	MV	MV-dnFOXO
State 3 respiration (nmoles O_2/mg/min)	12.0±0.8	8.8±0.9*	10.5±0.4
State 4 respiration (nmoles O_2/mg/min)	2.0±0.2	2.6±0.1*	2.6±0.1*
RCR	6.0±0.6	3.4±0.2*	4.1±0.2*

Values are expressed as mean ± SE. * Significantly different versus CON ($P<0.05$).

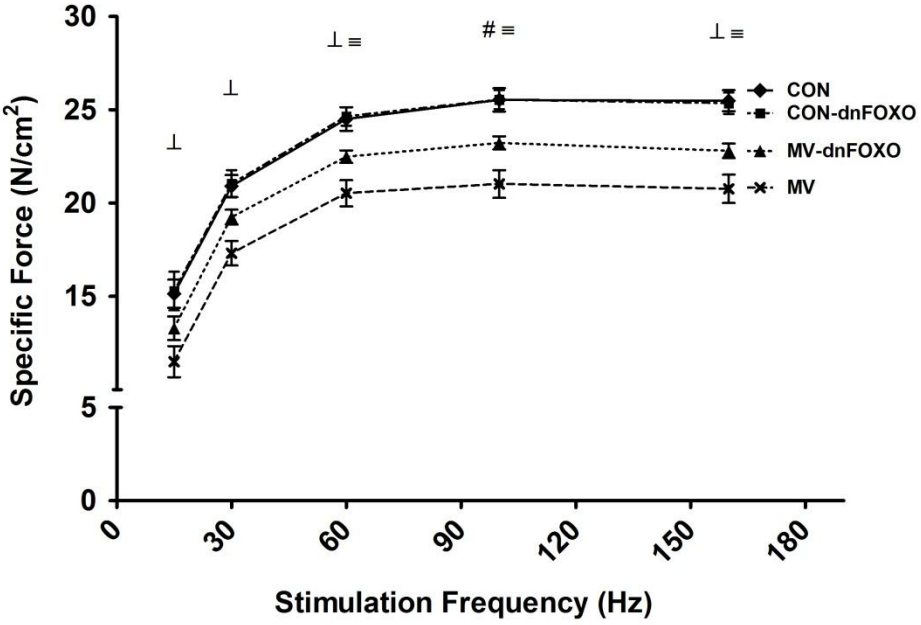

Figure 4-3. Diaphragm force-frequency response (*in vitro*) of diaphragm samples for experiment 1. Values are mean ± SE. ⊥ MV significantly different versus CON and CON-dnFOXO (P<0.05). ≡ MV-dnFOXO significantly different versus CON and Con-dnFOXO (P<0.05). # MV significantly different versus all groups (P<0.05).

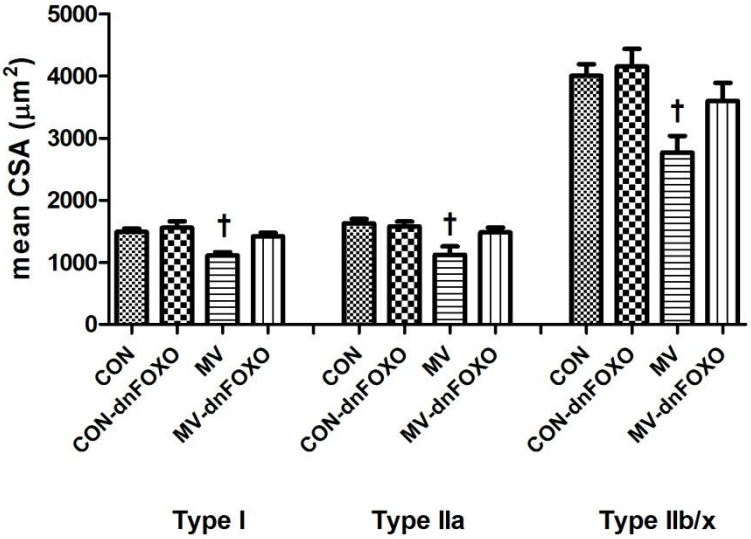

Figure 4-4. Diaphragm muscle cross-sectional area for experiment 1. Values are mean ± SE. † MV significantly different versus CON and CON-dnFOXO (P<0.05).

A) B)

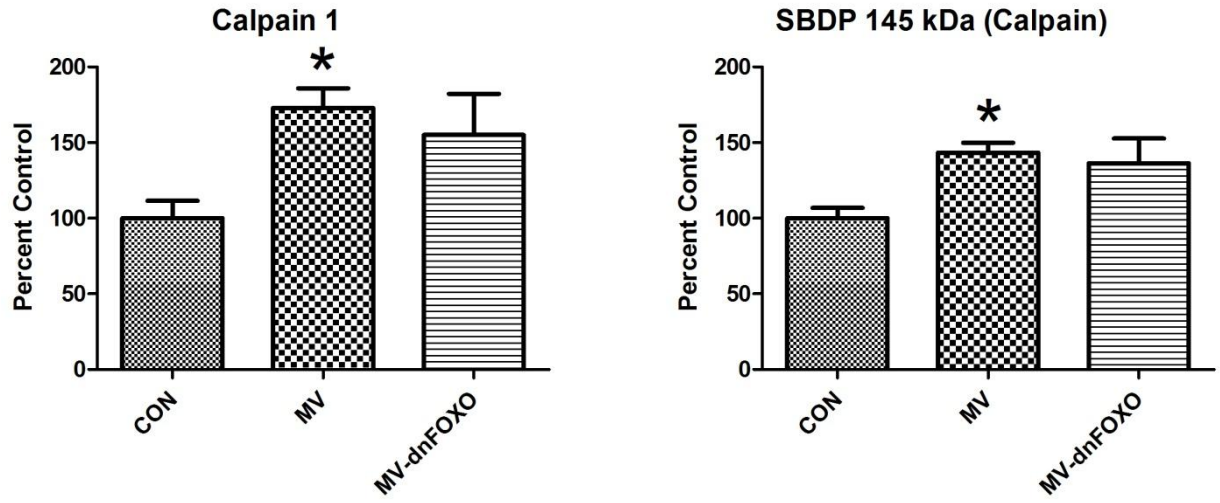

Figure 4-5. Calpain activation in diaphragm was determined via Western blotting for experiment 1. Values are mean ± SE. A) active Calpain 1 B) the calpain specific spectrin breakdown product (SBDP). * Significantly different versus CON (P<0.05).

A) B)

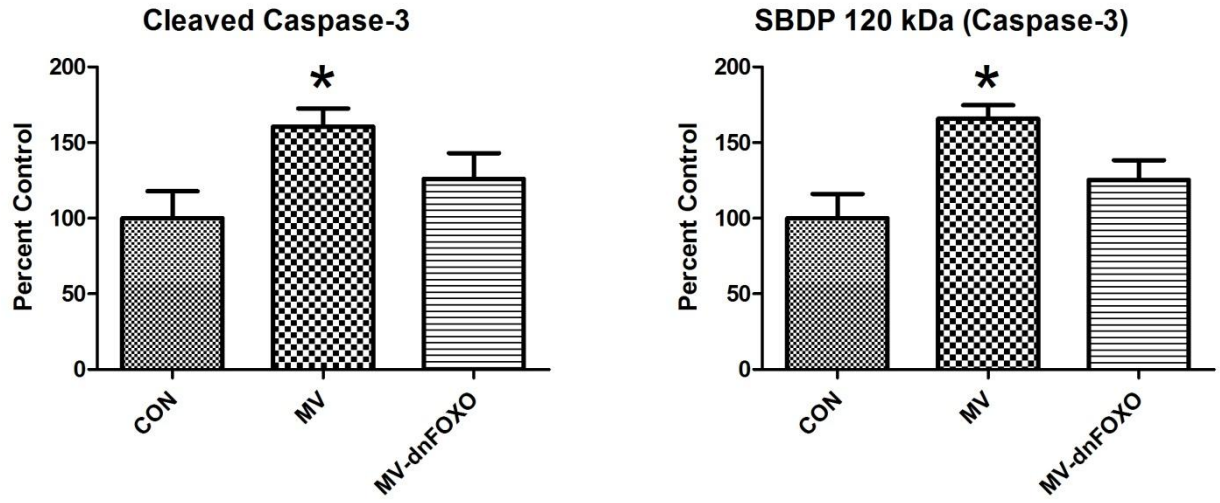

Figure 4-6. Caspase-3 activation in the diaphragm was determined via Western blotting for experiment 1. Values are mean ± SE. A) cleaved caspase-3 B) the caspase-3 specific spectrin breakdown product (SBDP). * Significantly different versus CON (P<0.05).

A) B)

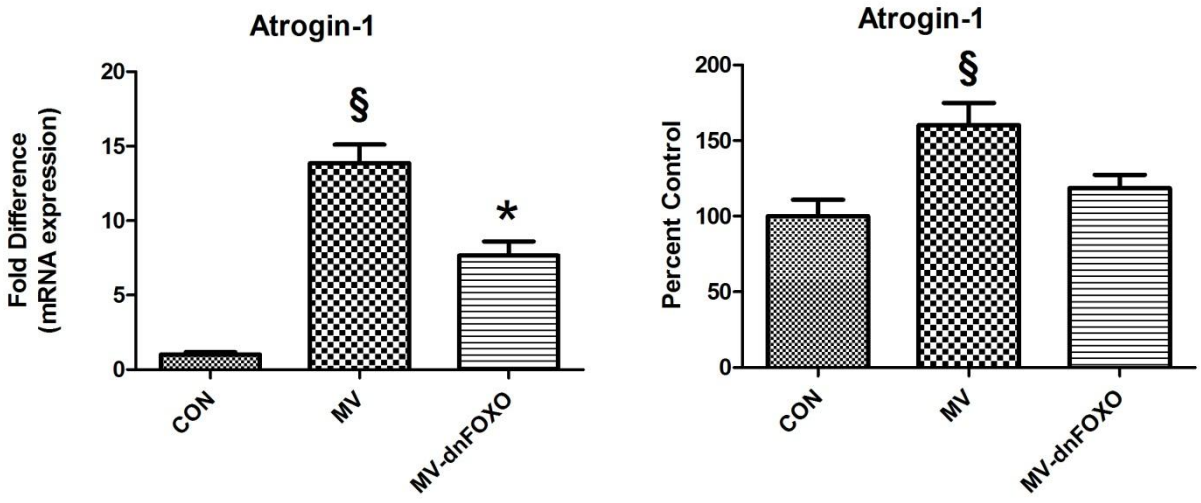

Figure 4-7. Atrogin-1 was measured as a marker of FOXO activity for experiment 1. Values are mean ± SE. A) Atrogin-1 mRNA expression B) Atrogin-1 protein expression. * Significantly different versus CON (P<0.05). § Significantly different versus all groups (P<0.05).

A) B)

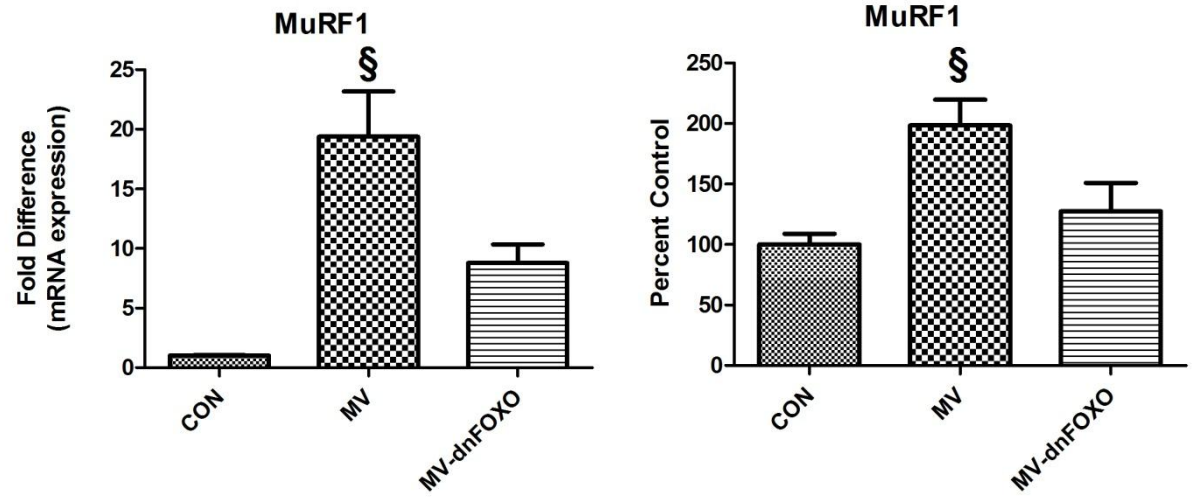

Figure 4-8. MuRF1 was measured as a marker of FOXO activity for experiment 1. Values are mean ± SE. A) MuRF1 mRNA expression B) MuRF1 protein expression. § Significantly different versus all groups (P<0.05).

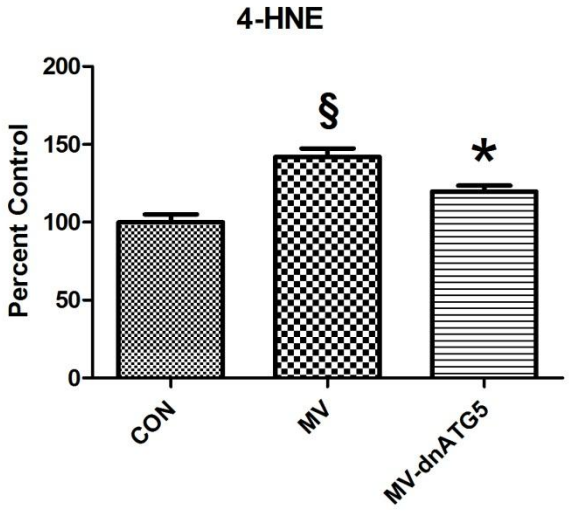

Figure 4-9. The levels of 4 hydroxynonenal (4-HNE) were analyzed as an indicator of lipid peroxidation via western blotting for experiment 2. Values are mean percentage change ± SE and normalized to α-tubulin. * Significantly different versus CON (P<0.05). § Significantly different versus all groups (P<0.05).

A) B)

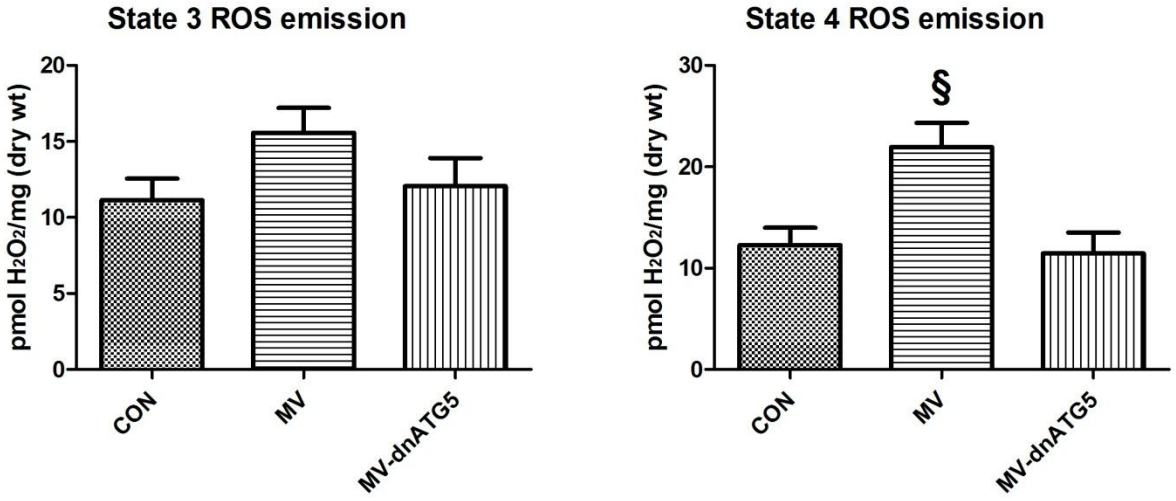

Figure 4-10. Rates of hydrogen peroxide release (H_2O_2) release from permeabilized diaphragm muscle fibers for experiment 2. Values are mean ± SE. A) State 3 ROS emission B) State 4 ROS emission. § Significantly different versus all groups (P<0.05).

Table 4-2. Mitochondrial respiratory function in permeabilized fibers from diaphragm muscle obtained from non-mechanically ventilated (CON), mechanically ventilated animals (MV) and mechanically ventilated animals with dnATG5 administration (MV-dnATG5).

	CON	MV	MV-dnATG5
State 3 respiration (nmoles O_2/mg/min)	12.0±1.1	8.8±0.5*	9.8±0.7
State 4 respiration (nmoles O_2/mg/min)	2.1±0.2	2.6±0.1§	2.0±0.1
RCR	6.0±0.4	3.4±0.1§	5.0±0.5

Values are expressed as mean ± SE. § Significantly different versus all groups ($P<0.05$). * Significantly different versus CON ($P<0.05$).

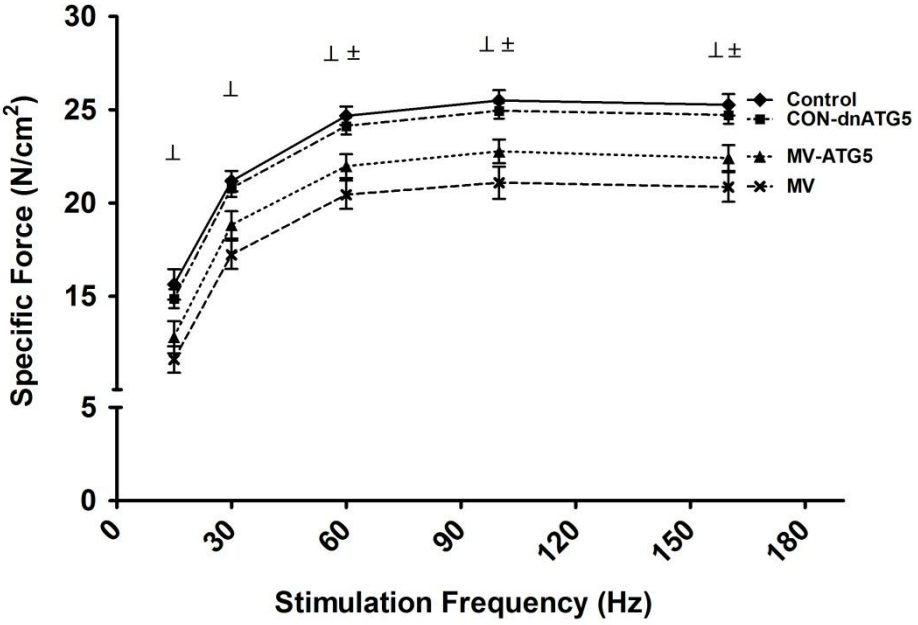

Figure 4-11. Diaphragm force-frequency response (*in vitro*) of diaphragm samples for experiment 2. Values are mean ± SE. ⊥ MV significantly different versus CON and CON-dnATG5 (P<0.05). ± MV-dnATG5 significantly different versus CON (P<0.05).

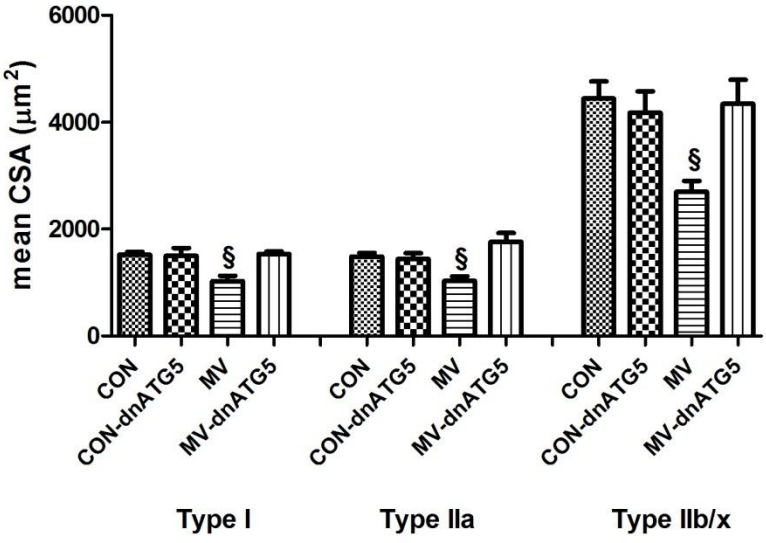

Figure 4-12. Diaphragm muscle cross-sectional area for experiment 1. Values are mean ± SE. § Significantly different versus all groups (P<0.05).

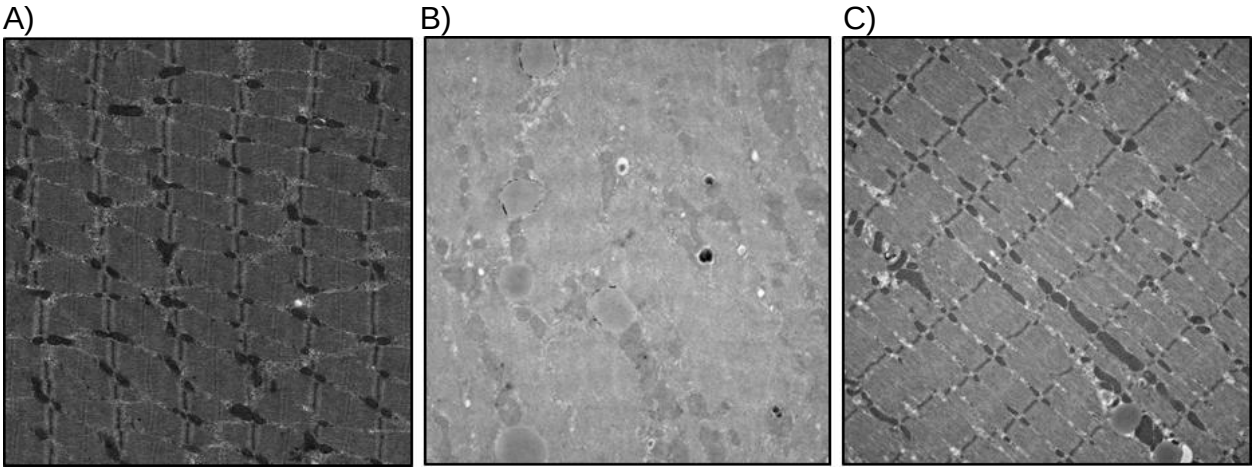

Figure 4-13. Electron microscopy representative images of diaphragm muscle obtained from animals in experiment 2. A) CON B) MV C) MV-dnATG5.

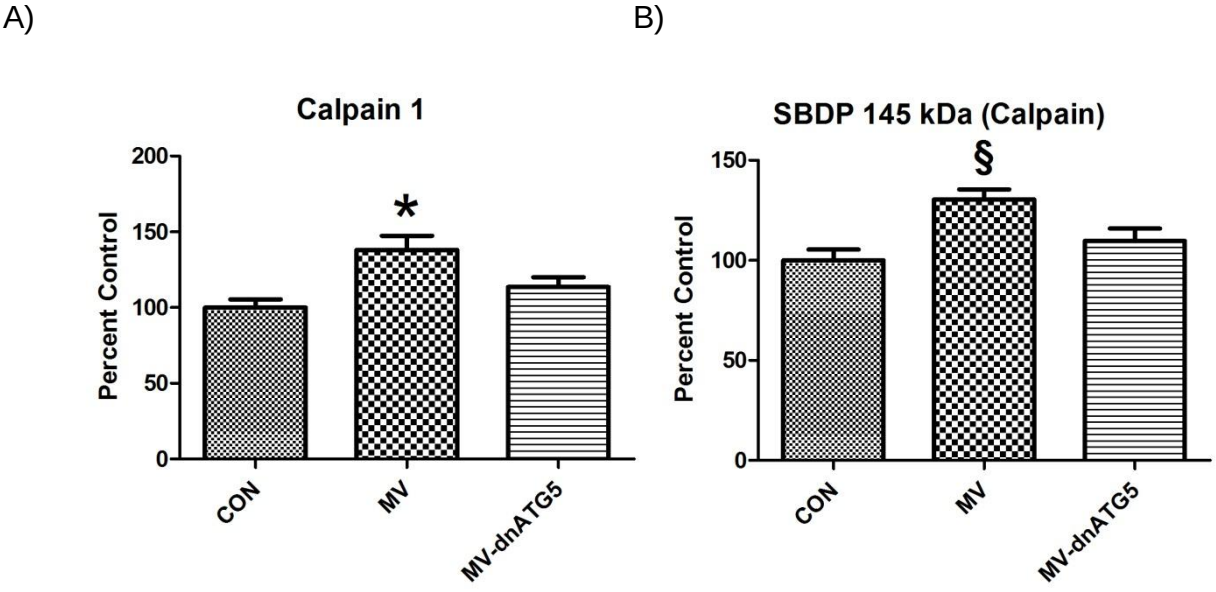

Figure 4-14. Calpain activation in diaphragm was determined via Western blotting for experiment 2. Values are mean ± SE. A) active Calpain 1 B) the calpain specific spectrin breakdown product (SBDP). * Significantly different versus CON ($P<0.05$).

A) B)

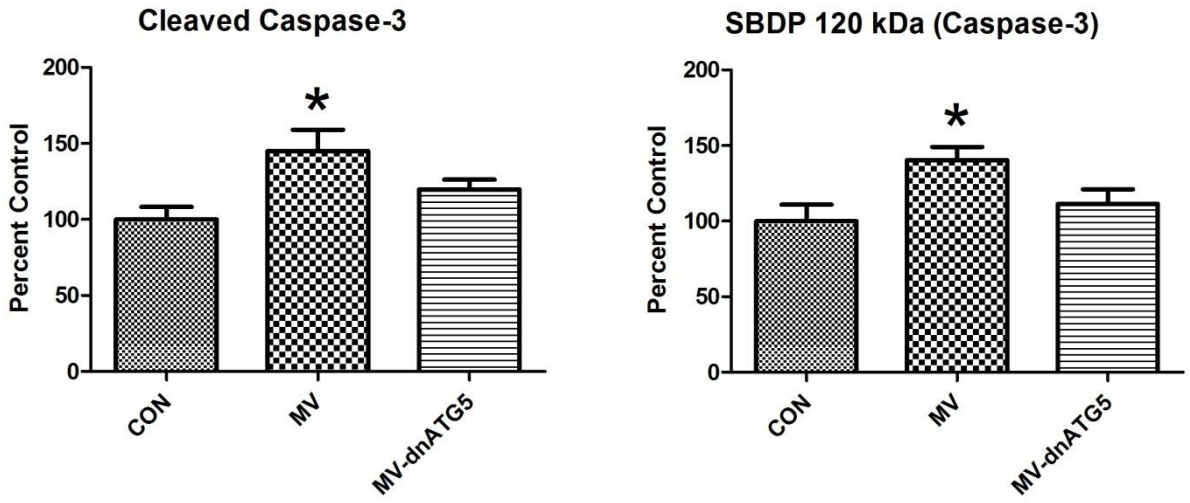

Figure 4-15. Caspase-3 activation in the diaphragm was determined via Western blotting for experiment 2. Values are mean ± SE. A) cleaved caspase-3 B) the caspase-3 specific spectrin breakdown product (SBDP). * Significantly different versus CON (P<0.05).

A) B)

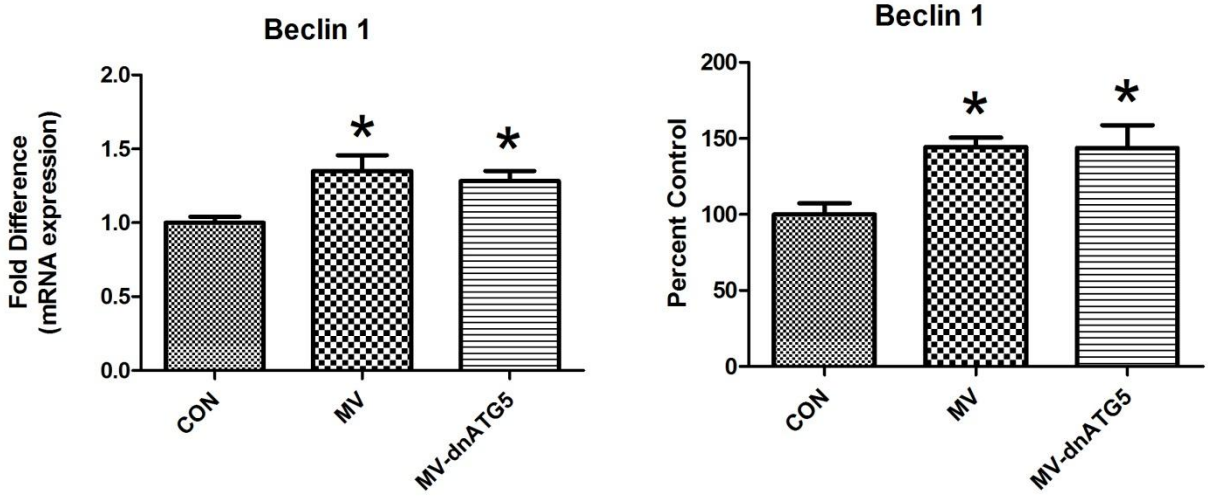

Figure 4-16. Beclin 1 was measured as a marker of the initiation of autophagosome formation for experiment 2. Values are mean ± SE. A) Beclin 1 mRNA expression B) Beclin 1 protein expression. * Significantly different versus CON (P<0.05).

A) B)

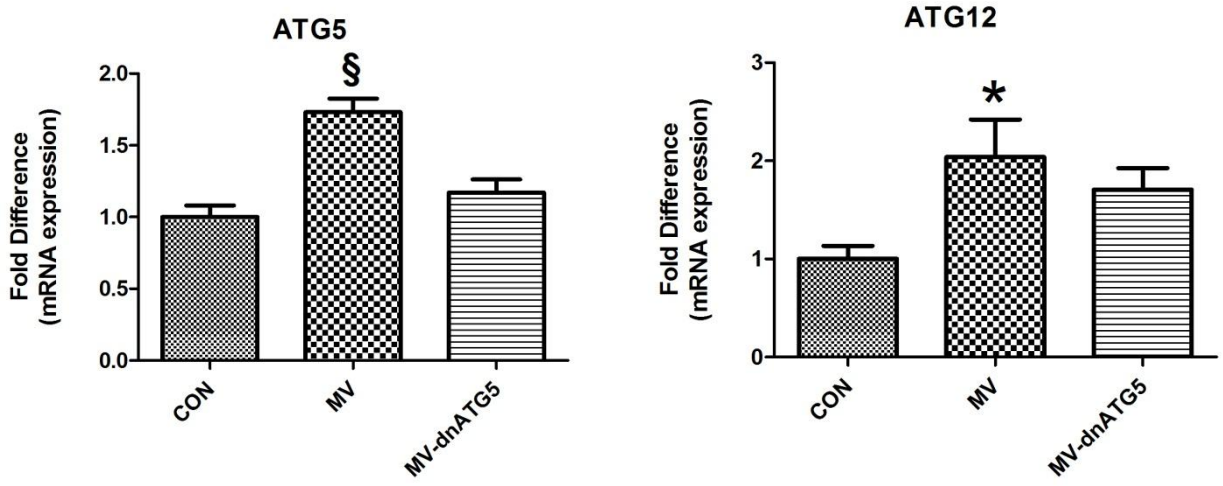

Figure 4-17. Atg5 and Atg12 were analyzed as markers of elongation of the autophagosome for experiment 2. Values are mean ± SE. A) Atg5 mRNA expression B) Atg12 mRNA expression. * Significantly different versus CON (P<0.05). § Significantly different versus all groups (P<0.05).

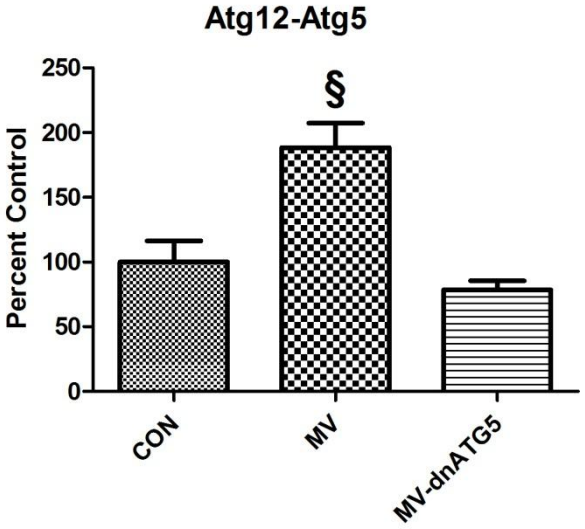

Figure 4-18. Atg12-Atg5 complex expression was measured via Western blotting as a marker of autophagosome formation for experiment 2. Values are mean ± SE. § Significantly different versus all groups (P<0.05).

A) B)

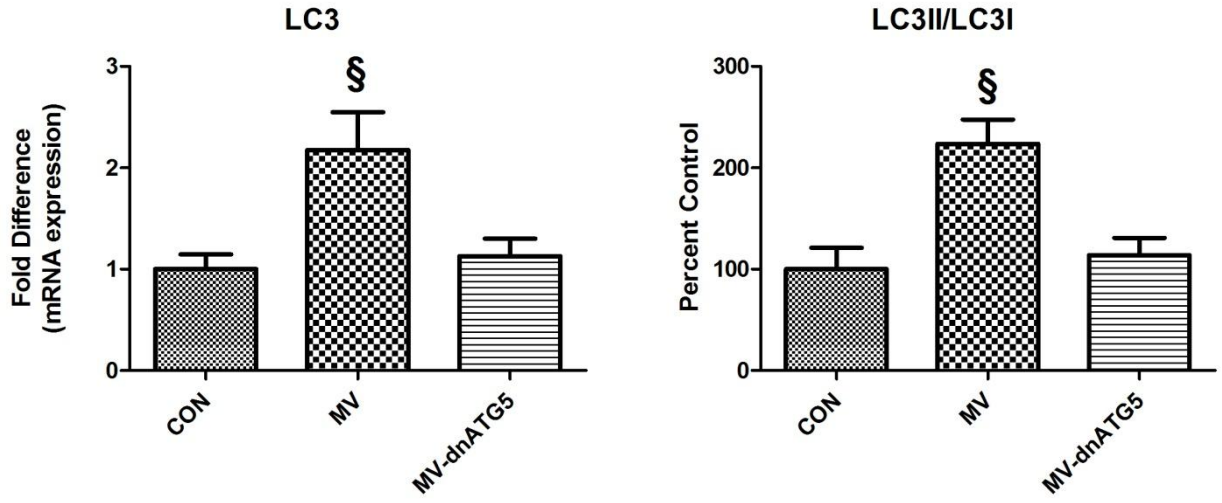

Figure 4-19. LC3 was measured as a marker of elongation and formation of the autophagosome for experiment 2. Values are mean ± SE. A) LC3 mRNA expression B) LC3II/LC3I ratio. § Significantly different versus all groups ($P<0.05$).

A) B) C)

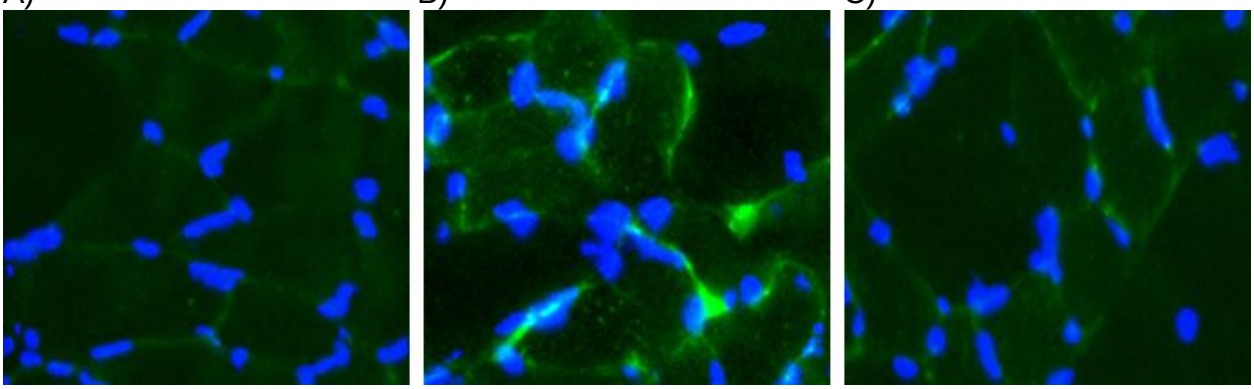

Figure 4-20. LC3 accumulation was examined in diaphragm muscle cross-sections for experiment 2. A) CON B) MV C) MV-dnFOXO. Blue represents dapi stained nuclei and green represents LC3.

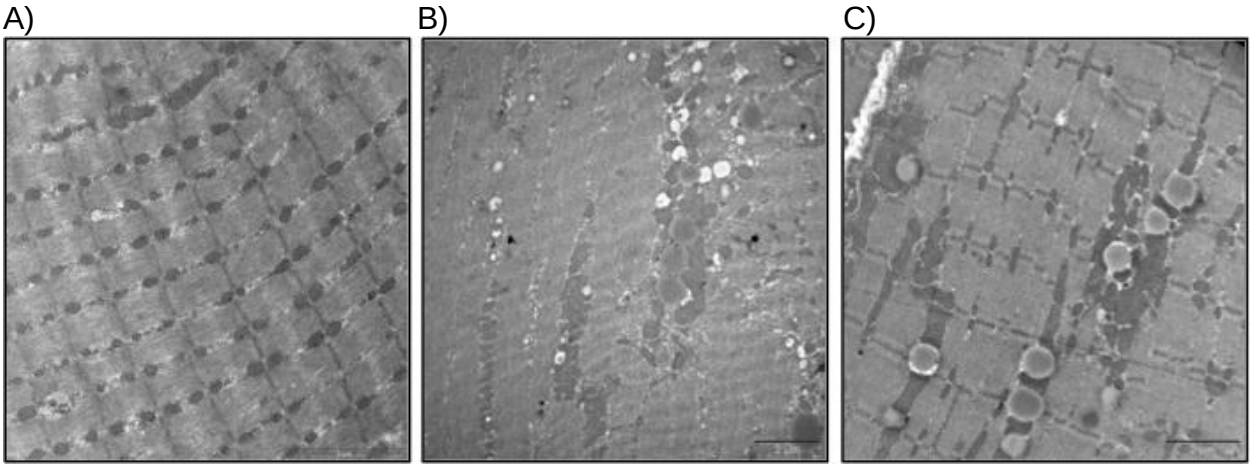

Figure 4-21. Electron microscopy representative images images of diaphragm muscle obtained from animals in experiment 3. A) CON B) MV C) MV-dnFOXO.

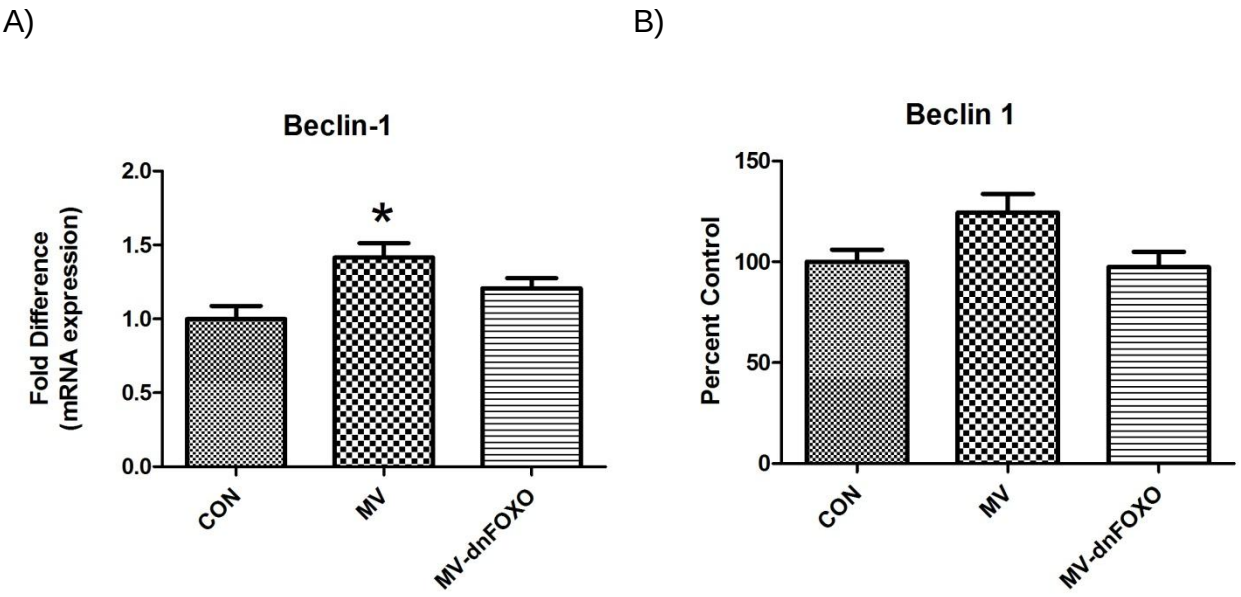

Figure 4-22. Beclin 1 was measured as a marker of the initiation of autophagosome formation for experiment 3. Values are mean ± SE. A) Beclin 1 mRNA expression B) Beclin 1 protein expression. * Significantly different versus CON ($P<0.05$).

A) B)

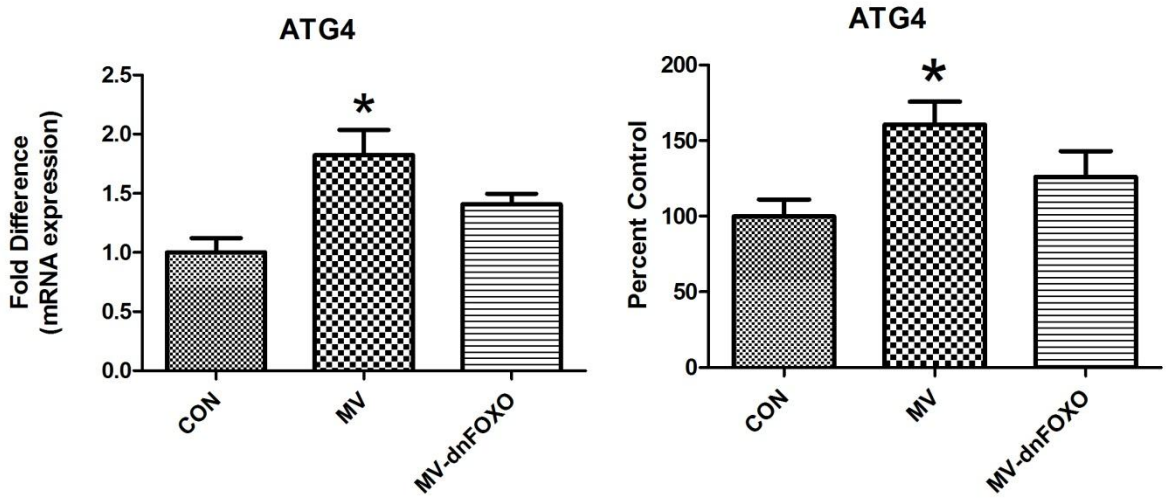

Figure 4-23. Atg4 was measured as a marker of the formation of the autophagosome for experiment 3. Values are mean ± SE. A) Atg4 mRNA expression B) Atg4 protein expression. * Significantly different versus CON (P<0.05).

A) B)

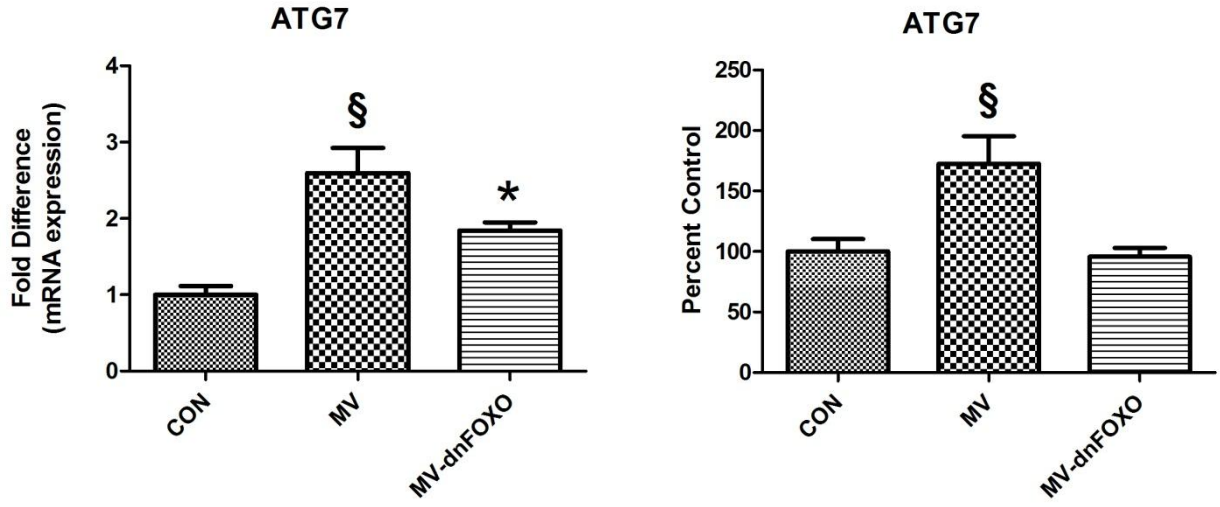

Figure 4-24. Atg7 was measured as a marker of the formation of the autophagosome for experiment 3. Values are mean ± SE. A) Atg7 mRNA expression B) Atg7 protein expression. * Significantly different versus CON (P<0.05). § Significantly different versus all groups (P<0.05).

A) B)

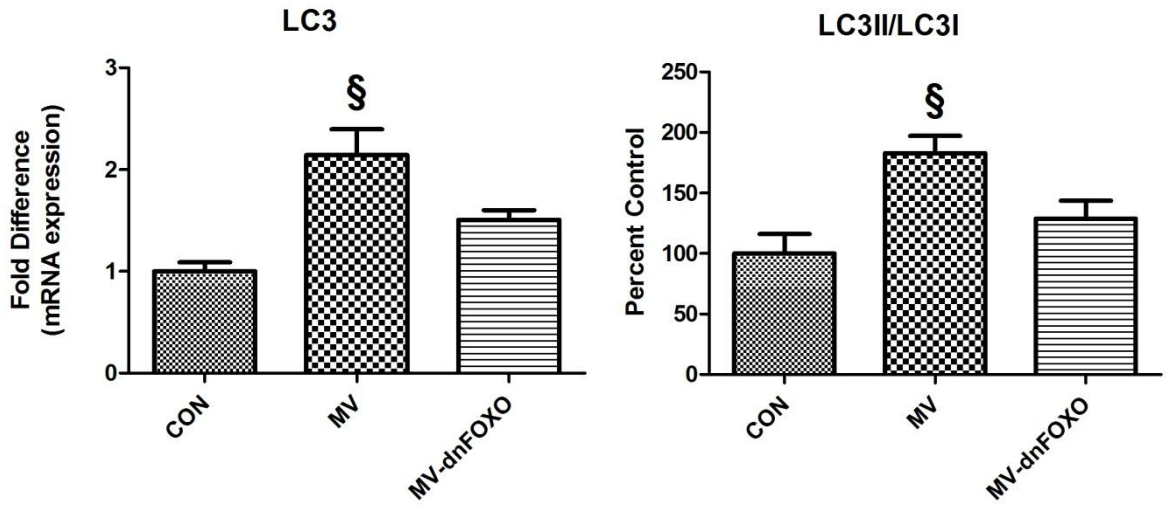

Figure 4-25. LC3 was measured as a marker of elongation and formation of the autophagosome for experiment 3. Values are mean ± SE. A) LC3 mRNA expression B) LC3II/LC3I ratio. § Significantly different versus all groups ($P<0.05$).

A) B) C)

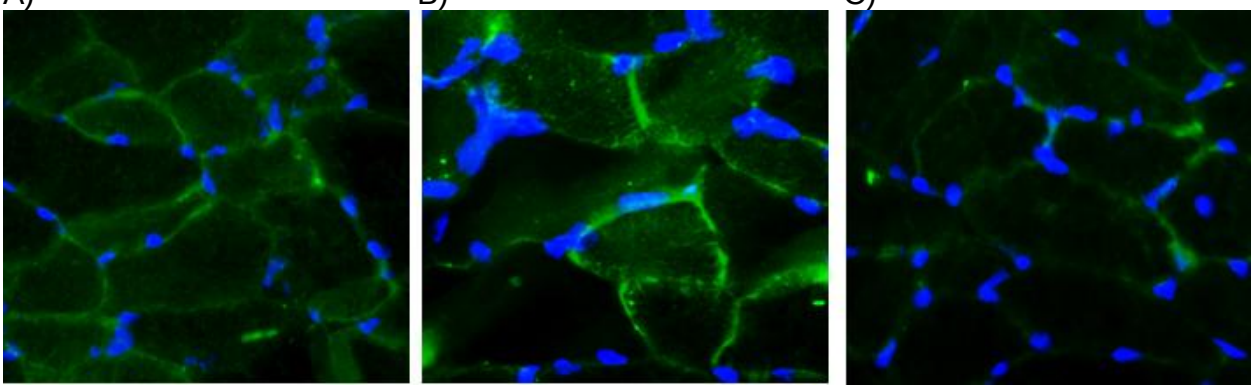

Figure 4-26. LC3 accumulation was examined in diaphragm muscle cross-sections for experiment 3. A) CON B) MV C) MV-dnATG5. Blue represents dapi stained nuclei and green represents LC3.

A) B)

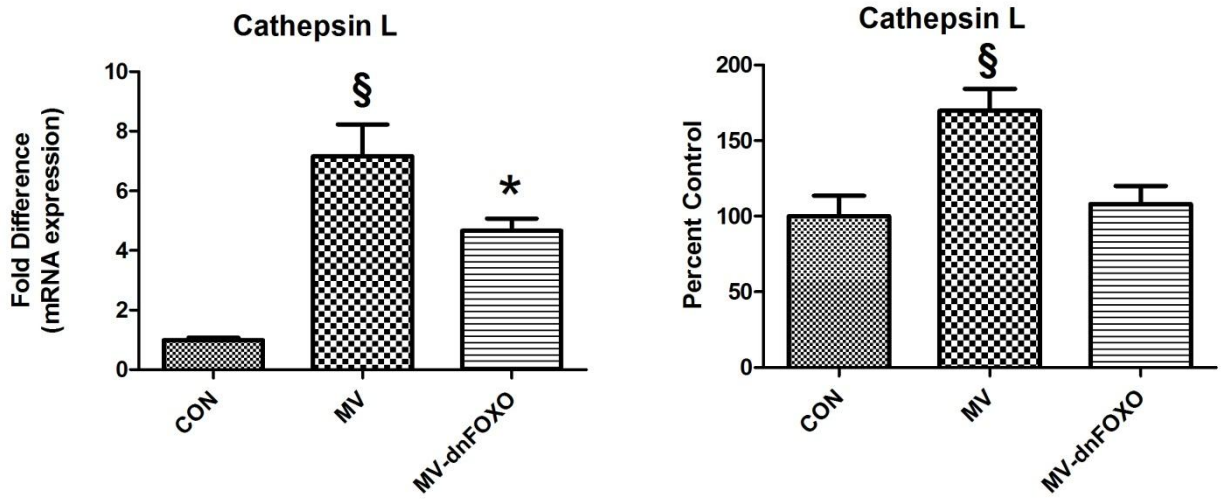

Figure 4-27. Cathepsin L was measured as a marker of increased degradation by the lysosomal proteolytic system for experiment 3. Values are mean ± SE. A) cathepsin L mRNA expression B) Cathepsin L protein expression. * Significantly different versus CON ($P<0.05$). § Significantly different versus all groups ($P<0.05$).

CHAPTER 5
DISCUSSION

Overview of Principal Findings

These experiments provide new and important information regarding the role that FOXO signaling and autophagy plays in ventilator-induced diaphragm dysfunction (VIDD). We tested the hypothesis that FOXO transcription is responsible for the activation of both proteasome-mediated proteolysis and autophagy, and that both FOXO transcription and autophagy contribute to mechanical ventilation (MV)-induced diaphragm atrophy and contractile dysfunction. Our novel findings reveal that both FOXO signaling and autophagy are increased in the diaphragm during prolonged MV. While both FOXO signaling and an upregulation of autophagy contribute to VIDD, autophagy appears to play a greater role in promoting VIDD compared to increased FOXO transcription alone. A detailed discussion of these findings follows.

MV-induced Induction of FOXO Transcription

The FOXO family of transcriptional activators consists of three members (FOXO1, FOXO3a and FOXO4). The importance of the FOXO-mediated signaling pathway has been shown during a variety of muscle wasting conditions (i.e. sepsis and cancer cachexia) and muscle-specific overexpression of FOXO1 or FOXO3a is sufficient to cause skeletal muscle atrophy *in vivo* (41, 46, 49). The regulation of muscle mass by FOXO transcription factors is thought to be due to the regulation of muscle atrophy-related genes. For example, Atrogin-1 and MuRF1 are two muscle specific E3 ligases whose expression is elevated during normal muscle wasting conditions (7, 41, 46). In addition, our current results and previous studies by our laboratory confirm that MV-induced diaphragmatic inactivity is a sufficient stimulus to cause an increase in the

expression of both Atrogin-1 and MuRF1 (37). In this regard, one objective of the current study was to determine whether FOXO signaling is responsible for the MV-induced increase in both Atrogin-1 and MuRF1 expression. Our results confirm that FOXO signaling is responsible for the increase in Atrogin-1 and MuRF1 and that through the use of a dnFOXO adeno-associated virus vector (AAV), we attenuated the increased expression of both proteins in the diaphragm during MV. This confirms that FOXO signaling does contribute to MV-induced activation of proteasome-mediated proteolysis.

FOXO Signaling Contributes to VIDD

Recent human studies along with work from our laboratory confirm that there is an increase in active FOXO in the diaphragm as a result of prolonged MV (18, 24, 29). Currently, the contribution of increased FOXO activity to VIDD is unknown. Using the dnFOXO AAV we were able to block FOXO binding sites in target genes, therefore preventing their transcriptional activation by endogenous FOXO (41). Compared to other disuse muscle wasting models, our data shows that FOXO signaling plays a lesser role in contributing to VIDD. In fact, our results demonstrate that blocking FOXO-specific gene transcription only partially attenuates the MV-induced diaphragm muscle atrophy and contractile dysfunction. Therefore, we speculate that FOXO activation may only be a downstream target of another essential proteolytic signaling mechanism.

In regard to FOXO activation, work by others has shown that FOXO may be a downstream target of the protease calpain (53). Additionally, work from our laboratory reveals that calpain signaling is required for MV-induced VIDD (26, 59). Therefore, calpain may act as an upstream trigger for the activation of Akt, which in turn activates FOXO. Based on this postulate we measured the activity of calpain in our experimental

groups. Our results show that calpain is indeed increased as a result of MV and our results also confirm that blocking FOXO transcription is not sufficient to reduce calpain activity. Therefore, it is possible that MV-induced calpain activation in the diaphragm may be required to activate FOXO during MV.

In addition to calpain activation, mitochondrial ROS production has been shown to be an upstream trigger that leads to MV-induced increases in atrophy and contractile dysfunction (19, 37). In fact, our laboratory has shown that treatment of animals with a mitochondrial-targeted antioxidant is sufficient to protect the diaphragm from VIDD (37). In the current study we also determined that MV promotes a significant increase in diaphragmatic mitochondrial H_2O_2 emission as well as a decrease in the RCR. This confirms that MV causes mitochondrial dysfunction and that this mitochondrial damage occurs upstream of FOXO activation. Therefore, mitochondrial oxidative damage and/or increased mitochondrial H_2O_2 emission may also be a stimulus to active FOXO during MV.

MV-induced Induction of Autophagy

Prolonged MV results in the activation of many different proteolytic signaling pathways in the diaphragm, and recently it was revealed that prolonged MV promotes an increase in the expression of many autophagy genes and the lysosomal protease cathepsin L in the diaphragms of human patients (18). While basal autophagy is necessary for cell survival, excessive autophagy results in significant muscle atrophy (18, 27, 34). Specifically, the induction of autophagy involves the formation of a small isolation membrane, which is elongated to form a mature autophagosome. Autophagosome formation is regulated by a system of autophagy proteins, many of which are increased in the diaphragm during MV (18). In this regard, our objective was

to determine the role of autophagy in MV-induced diaphragm muscle wasting by altering a key component of autophagosome formation. To prevent MV-induced increases in autophagy we transfected the diaphragm with a dominant negative mutant of Atg5. Specifically, this mutated form of Atg5 is defective in its conjugation to Atg12, which is required for LC3 incorporation into the early autophagosomal structure, and thus inhibits autophagy at the level of autophagosome formation (16). To confirm the inhibitory nature of the vector we measured the levels of Atg12 bound to Atg5 in the diaphragm. Our data indicates that MV results in an increase in the protein levels of Atg12 bound to Atg5 in the diaphragm, and also confirms that administration of the dnATG5 was sufficient to knockdown the amount of Atg12 bound to Atg5. In addition, we also measured the ratio of LC3 II to LC3 I and examined the relative abundance of LC3 in diaphragm muscle cross-sections to confirm that our vector did indeed inhibit autophagy during MV. In agreement with the Atg12-Atg5 protein measurement, the ratio of LC3 II to LC3I was also decreased during MV as a result of administration of the dnATG5 and we also confirmed that the dnATG5 was responsible for a decrease in the accumulation of LC3 in diaphragm muscle fibers of mechanically ventilated animals. In addition to these measures, electron microscopy images obtained from our experimental groups also confirm that treatment with the dnATG5 protects the diaphragm against MV-induced autophagosome formation/lipid accumulation as well as the preservation of normal diaphragm sarcomeric structure.

Autophagy Contributes to VIDD

Autophagy is upregulated during conditions of muscle catabolism. While it appears that autophagy is critical for normal muscle function, increased autophagic flux can induce muscle atrophy (44). Our data confirms this postulate, as MV results in both an

increase in autophagy signaling and increased atrophy in the diaphragm. In this regard, animals that were treated with the dnATG5 demonstrated a reduction in autophagy and the diaphragms of these animals were protected against MV-induced atrophy. In contrast, diaphragm muscle functional measurements demonstrated prolonged MV resulted in a significant decrease in diaphragm muscle specific force production and inhibiting autophagy did not provide significant protection against the MV-induced decline in diaphragmatic contractile performance. This disparity may be attributed to an accumulation of proteins within the muscle due to the inhibition of autophagy-mediated degradation of proteins.

FOXO and Autophagy

As previously described, FOXO transcription factors contribute to skeletal muscle atrophy by increasing the transcription of several key proteins of the proteasome system of proteolysis. However, in addition to a role in the increased expression of proteasome proteins leading to myofibrillar degradation, FOXO activation has also been shown to be sufficient for the induction of autophagy in skeletal muscle (27). Specifically, FOXO controls the transcription of key autophagy related genes, including LC3 and Cathepsin L (27, 41). The effect of FOXO on autophagy appears to be independent of FOXO's interaction with the proteasome. Therefore, it is possible that FOXO may independently control two major systems of skeletal muscle protein breakdown.

During autophagy, the cytoplasmic form of LC3 (LC3 I) is recruited to the autophagosome where LC3 II is generated. The formation of LC3 II compared to LC3 I is used as a marker or autophagic activity as well as the accumulation of LC3 within the muscle fibers. Blocking FOXO transcription not only reduced the expression of LC3, it also resulted in a decrease in the ratio of LC3II to LC3 I in diaphragms of mechanically

ventilated animals. However, electron microscopy images from these animals determined that there is only a small reduction of autophagic vacuole formation in the diaphragm when FOXO signaling is blocked. To determine the effect of FOXO signaling on autophagy we also measured the expression of several other autophagy proteins in diaphragms from control and mechanically ventilated animals. Specifically, we measured the expression of Beclin 1, Atg7 and Atg4 to confirm that MV results in an increase in autophagy. Our results show that there is a MV-induced increase in the expression of these proteins in the diaphragm and that use of the dnFOXO was able to attenuate the increase in both Atg7 and Atg4. This is significant because LC3 interacts with both of these proteins for the expansion and completion of the autophagosome.

Once the autophagsome is complete, lysosomes containing numerous proteases (i.e. cathepsins) fuse with the autophagsome to create the autolysosome (33). It has been reported that during conditions of muscle damage there is an increase in the expression of cathepsins in muscle fibers (4, 56). Cathepsin L is a lysosomal protease that is expressed in skeletal muscle during wasting conditions and it is also a transcriptional target of FOXO (41, 60). Our data shows that MV results in a significant increase in cathepsin L expression and that expression of dnFOXO significantly reduces its expression compared to MV. Therefore, our results support the postulate that FOXO signaling is responsible for controlling signaling of the autophagy/lysosomal system during MV.

In addition to FOXO's ability to activate autophagy through the transcription of several autophagy genes, oxidative stress has also been shown to independently increase signaling of the autophagy/lysosomal system. In this regard, our results show

that treatment of the diaphragm with dnFOXO was sufficient to prevent the MV-induced increases in mitochondrial H_2O_2 emission. Therefore, it is possible that FOXO's partial rescue of the diaphragm from increased autophagy is due to FOXO's influence on reactive oxygen species production. These results are consistent with the concept that FOXO signaling is not the primary upstream trigger controlling MV-induced diaphragmatic atrophy.

Conclusions and Future Directions

This study provides the first evidence regarding the role that FOXO and autophagy signaling play in contributing to MV-induced diaphragm weakness. Specifically, these results demonstrate that FOXO signaling in the diaphragm during MV is responsible for the upregulation of components of both the ubiquitin-proteasome system of proteolysis and the autophagy/lysosomal system. Furthermore, our data also reveals that FOXO signaling only partially contributes to the increased diaphragmatic atrophy and contractile dysfunction seen as a result of prolonged MV. Importantly, our findings also suggest that autophagy signaling is regulated by increases in ROS and inhibition of autophagy is able to provide protection against MV-induced diaphragmatic atrophy.

Finally, although the current studies do not provide a clinically relevant treatment for VIDD, these studies are the first to use AAV in the diaphragm of rats to help combat skeletal muscle wasting. Importantly, these experiments have identified two important biological targets for therapeutic intervention to prevent MV-induced diaphragmatic atrophy. Prevention of MV-induced diaphragmatic weakness is important because inspiratory muscle weakness is known to be a major contributor to difficult weaning.

LIST OF REFERENCES

1. **Anzueto A, Peters JI, Tobin MJ, de los Santos R, Seidenfeld JJ, Moore G, Cox WJ, and Coalson JJ**. Effects of prolonged controlled mechanical ventilation on diaphragmatic function in healthy adult baboons. *Crit Care Med* 25: 1187-1190, 1997.
2. **Attaix D, Ventadour S, Codran A, Bechet D, Taillandier D, and Combaret L**. The ubiquitin-proteasome system and skeletal muscle wasting. *Essays Biochem* 41: 173-186, 2005.
3. **Baar K, Nader G, and Bodine S**. Resistance exercise, muscle loading/unloading and the control of muscle mass. *Essays Biochem* 42: 61-74, 2006.
4. **Bechet D, Tassa A, Taillandier D, Combaret L, and Attaix D**. Lysosomal proteolysis in skeletal muscle. *Int J Biochem Cell Biol* 37: 2098-2114, 2005.
5. **Bernard N, Matecki S, Py G, Lopez S, Mercier J, and Capdevila X**. Effects of prolonged mechanical ventilation on respiratory muscle ultrastructure and mitochondrial respiration in rabbits. *Intensive Care Med* 29: 111-118, 2003.
6. **Betters JL, Criswell DS, Shanely RA, Van Gammeren D, Falk D, Deruisseau KC, Deering M, Yimlamai T, and Powers SK**. Trolox attenuates mechanical ventilation-induced diaphragmatic dysfunction and proteolysis. *Am J Respir Crit Care Med* 170: 1179-1184, 2004.
7. **Bodine SC, Latres E, Baumhueter S, Lai VK, Nunez L, Clarke BA, Poueymirou WT, Panaro FJ, Na E, Dharmarajan K, Pan ZQ, Valenzuela DM, DeChiara TM, Stitt TN, Yancopoulos GD, and Glass DJ**. Identification of ubiquitin ligases required for skeletal muscle atrophy. *Science* 294: 1704-1708, 2001.
8. **Deruisseau KC, Kavazis AN, and Powers SK**. Selective downregulation of ubiquitin conjugation cascade mRNA occurs in the senescent rat soleus muscle. *Exp Gerontol* 40: 526-531, 2005.
9. **DeRuisseau KC, Shanely RA, Akunuri N, Hamilton MT, Van Gammeren D, Zergeroglu AM, McKenzie M, and Powers SK**. Diaphragm unloading via controlled mechanical ventilation alters the gene expression profile. *Am J Respir Crit Care Med* 172: 1267-1275, 2005.
10. **Du J, Wang X, Miereles C, Bailey JL, Debigare R, Zheng B, Price SR, and Mitch WE**. Activation of caspase-3 is an initial step triggering accelerated muscle proteolysis in catabolic conditions. *J Clin Invest* 113: 115-123, 2004.
11. **Esteban A, Alia I, Ibanez J, Benito S, and Tobin MJ**. Modes of mechanical ventilation and weaning. A national survey of Spanish hospitals. The Spanish Lung Failure Collaborative Group. *Chest* 106: 1188-1193, 1994.
12. **Esteban A, Anzueto A, Alia I, Gordo F, Apezteguia C, Palizas F, Cide D, Goldwaser R, Soto L, Bugedo G, Rodrigo C, Pimentel J, Raimondi G, and Tobin MJ**. How is mechanical ventilation employed in the intensive care unit? An international utilization review. *Am J Respir Crit Care Med* 161: 1450-1458, 2000.
13. **Falk DJ, Deruisseau KC, Van Gammeren DL, Deering MA, Kavazis AN, and Powers SK**. Mechanical ventilation promotes redox status alterations in the diaphragm. *J Appl Physiol* 101: 1017-1024, 2006.

14. **Fredriksson K, Radell P, Eriksson LI, Hultenby K, and Rooyackers O**. Effect of prolonged mechanical ventilation on diaphragm muscle mitochondria in piglets. *Acta Anaesthesiol Scand* 49: 1101-1107, 2005.
15. **Goll DE, Thompson VF, Li H, Wei W, and Cong J**. The calpain system. *Physiol Rev* 83: 731-801, 2003.
16. **Hamacher-Brady A, Brady NR, and Gottlieb RA**. Enhancing macroautophagy protects against ischemia/reperfusion injury in cardiac myocytes. *J Biol Chem* 281: 29776-29787, 2006.
17. **Hess D**. Essentials of Mechanical Ventilation. *New York: McGraw-Hill* 1996.
18. **Hussain SN, Mofarrahi M, Sigala I, Kim HC, Vassilakopoulos T, Maltais F, Bellenis I, Chaturvedi R, Gottfried SB, Metrakos P, Danialou G, Matecki S, Jaber S, Petrof BJ, and Goldberg P**. Mechanical ventilation-induced diaphragm disuse in humans triggers autophagy. *Am J Respir Crit Care Med* 182: 1377-1386.
19. **Kavazis AN, Talbert EE, Smuder AJ, Hudson MB, Nelson WB, and Powers SK**. Mechanical ventilation induces diaphragmatic mitochondrial dysfunction and increased oxidant production. *Free Radic Biol Med* 46: 842-850, 2009.
20. **Knisely AS, Leal SM, and Singer DB**. Abnormalities of diaphragmatic muscle in neonates with ventilated lungs. *J Pediatr* 113: 1074-1077, 1988.
21. **Laghi F, Cattapan SE, Jubran A, Parthasarathy S, Warshawsky P, Choi YS, and Tobin MJ**. Is weaning failure caused by low-frequency fatigue of the diaphragm? *Am J Respir Crit Care Med* 167: 120-127, 2003.
22. **Le Bourdelles G, Viires N, Boczkowski J, Seta N, Pavlovic D, and Aubier M**. Effects of mechanical ventilation on diaphragmatic contractile properties in rats. *Am J Respir Crit Care Med* 149: 1539-1544, 1994.
23. **Lemaire F**. Difficult Weaning. *Intensive Care Med* 19 Suppl 2: S69-73: 1993.
24. **Levine S, Biswas C, Dierov J, Barsotti R, Shrager JB, Nguyen T, Sonnad S, Kucharchzuk JC, Kaiser LR, Singhal S, and Budak MT**. Increased proteolysis, myosin depletion, and atrophic AKT-FOXO signaling in human diaphragm disuse. *Am J Respir Crit Care Med* 183: 483-490, 2011.
25. **Levine S, Nguyen T, Taylor N, Friscia ME, Budak MT, Rothenberg P, Zhu J, Sachdeva R, Sonnad S, Kaiser LR, Rubinstein NA, Powers SK, and Shrager JB**. Rapid disuse atrophy of diaphragm fibers in mechanically ventilated humans. *N Engl J Med* 358: 1327-1335, 2008.
26. **Maes K, Testelmans D, Powers S, Decramer M, and Gayan-Ramirez G**. Leupeptin inhibits ventilator-induced diaphragm dysfunction in rats. *Am J Respir Crit Care Med* 175: 1134-1138, 2007.
27. **Mammucari C, Milan G, Romanello V, Masiero E, Rudolf R, Del Piccolo P, Burden SJ, Di Lisi R, Sandri C, Zhao J, Goldberg AL, Schiaffino S, and Sandri M**. FoxO3 controls autophagy in skeletal muscle in vivo. *Cell Metab* 6: 458-471, 2007.
28. **McClung JM, Kavazis AN, DeRuisseau KC, Falk DJ, Deering MA, Lee Y, Sugiura T, and Powers SK**. Caspase-3 regulation of diaphragm myonuclear domain during mechanical ventilation-induced atrophy. *Am J Respir Crit Care Med* 175: 150-159, 2007.

29. **McClung JM, Kavazis AN, Whidden MA, DeRuisseau KC, Falk DJ, Criswell DS, and Powers SK**. Antioxidant administration attenuates mechanical ventilation-induced rat diaphragm muscle atrophy independent of protein kinase B (PKB Akt) signalling. *J Physiol* 585: 203-215, 2007.
30. **Messer JI, Jackman MR, and Willis WT**. Pyruvate and citric acid cycle carbon requirements in isolated skeletal muscle mitochondria. *Am J Physiol Cell Physiol* 286: C565-572, 2004.
31. **Metzger JM, Scheidt KB, and Fitts RH**. Histochemical and physiological characteristics of the rat diaphragm. *J Appl Physiol* 58: 1085-1091, 1985.
32. **Mizuno M**. Human respiratory muscles: fibre morphology and capillary supply. *Eur Respir J* 4: 587-601, 1991.
33. **Mizushima N**. Autophagy: process and function. *Genes Dev* 21: 2861-2873, 2007.
34. **O'Leary MF, and Hood DA**. Denervation-induced oxidative stress and autophagy signaling in muscle. *Autophagy* 5: 230-231, 2009.
35. **Poole DC, Sexton WL, Farkas GA, Powers SK, and Reid MB**. Diaphragm structure and function in health and disease. *Med Sci Sports Exerc* 29: 738-754, 1997.
36. **Powers SK, Demirel HA, Coombes JS, Fletcher L, Calliaud C, Vrabas I, and Prezant D**. Myosin phenotype and bioenergetic characteristics of rat respiratory muscles. *Med Sci Sports Exerc* 29: 1573-1579, 1997.
37. **Powers SK, Hudson MB, Nelson WB, Talbert EE, Min K, Szeto HH, Kavazis AN, and Smuder AJ**. Mitochondria-targeted antioxidants protect against mechanical ventilation-induced diaphragm weakness. *Crit Care Med* 39: 1749-1759.
38. **Powers SK, Kavazis AN, and DeRuisseau KC**. Mechanisms of disuse muscle atrophy: role of oxidative stress. *Am J Physiol Regul Integr Comp Physiol* 288: R337-344, 2005.
39. **Powers SK, Shanely RA, Coombes JS, Koesterer TJ, McKenzie M, Van Gammeren D, Cicale M, and Dodd SL**. Mechanical ventilation results in progressive contractile dysfunction in the diaphragm. *J Appl Physiol* 92: 1851-1858, 2002.
40. **Radell PJ, Remahl S, Nichols DG, and Eriksson LI**. Effects of prolonged mechanical ventilation and inactivity on piglet diaphragm function. *Intensive Care Med* 28: 358-364, 2002.
41. **Reed SA, Sandesara PB, Senf SM, and Judge AR**. Inhibition of FoxO transcriptional activity prevents muscle fiber atrophy during cachexia and induces hypertrophy. *FASEB J* 2011.
42. **Reed SA, Senf SM, Cornwell EW, Kandarian SC, and Judge AR**. Inhibition of IkappaB kinase alpha (IKKalpha) or IKKbeta (IKKbeta) plus forkhead box O (Foxo) abolishes skeletal muscle atrophy. *Biochem Biophys Res Commun* 405: 491-496.
43. **Reid MB**. Free radicals and muscle fatigue: Of ROS, canaries, and the IOC. *Free Radic Biol Med* 44: 169-179, 2008.
44. **Sandri M**. Autophagy in health and disease. 3. Involvement of autophagy in muscle atrophy. *Am J Physiol Cell Physiol* 298: C1291-1297, 2010.

45. **Sandri M**. Autophagy in skeletal muscle. *FEBS Lett* 584: 1411-1416.
46. **Sandri M, Sandri C, Gilbert A, Skurk C, Calabria E, Picard A, Walsh K, Schiaffino S, Lecker SH, and Goldberg AL**. Foxo transcription factors induce the atrophy-related ubiquitin ligase atrogin-1 and cause skeletal muscle atrophy. *Cell* 117: 399-412, 2004.
47. **Sassoon CS**. Ventilator-associated diaphragmatic dysfunction. *Am J Respir Crit Care Med* 166: 1017-1018, 2002.
48. **Segal SS, White TP, and Faulkner JA**. Architecture, composition, and contractile properties of rat soleus muscle grafts. *Am J Physiol* 250: C474-479, 1986.
49. **Senf SM, Dodd SL, and Judge AR**. FOXO signaling is required for disuse muscle atrophy and is directly regulated by Hsp70. *Am J Physiol Cell Physiol* 298: C38-45, 2010.
50. **Shanely RA, Coombes JS, Zergeroglu AM, Webb AI, and Powers SK**. Short-duration mechanical ventilation enhances diaphragmatic fatigue resistance but impairs force production. *Chest* 123: 195-201, 2003.
51. **Shanely RA, Van Gammeren D, Deruisseau KC, Zergeroglu AM, McKenzie MJ, Yarasheski KE, and Powers SK**. Mechanical ventilation depresses protein synthesis in the rat diaphragm. *Am J Respir Crit Care Med* 170: 994-999, 2004.
52. **Shanely RA, Zergeroglu MA, Lennon SL, Sugiura T, Yimlamai T, Enns D, Belcastro A, and Powers SK**. Mechanical ventilation-induced diaphragmatic atrophy is associated with oxidative injury and increased proteolytic activity. *Am J Respir Crit Care Med* 166: 1369-1374, 2002.
53. **Smith IJ, and Dodd SL**. Calpain activation causes a proteasome-dependent increase in protein degradation and inhibits the Akt signalling pathway in rat diaphragm muscle. *Exp Physiol* 92: 561-573, 2007.
54. **Smith IJ, Lecker SH, and Hasselgren PO**. Calpain activity and muscle wasting in sepsis. *Am J Physiol Endocrinol Metab* 295: E762-771, 2008.
55. **Taillandier D, Combaret L, Pouch MN, Samuels SE, Bechet D, and Attaix D**. The role of ubiquitin-proteasome-dependent proteolysis in the remodelling of skeletal muscle. *Proc Nutr Soc* 63: 357-361, 2004.
56. **Turk V, Turk B, and Turk D**. Lysosomal cysteine proteases: facts and opportunities. *EMBO J* 20: 4629-4633, 2001.
57. **Van Gammeren D, Falk DJ, DeRuisseau KC, Sellman JE, Decramer M, and Powers SK**. Reloading the diaphragm following mechanical ventilation does not promote injury. *Chest* 127: 2204-2210, 2005.
58. **Watson AC, Hughes PD, Louise Harris M, Hart N, Ware RJ, Wendon J, Green M, and Moxham J**. Measurement of twitch transdiaphragmatic, esophageal, and endotracheal tube pressure with bilateral anterolateral magnetic phrenic nerve stimulation in patients in the intensive care unit. *Crit Care Med* 29: 1325-1331, 2001.
59. **Whidden MA, Smuder AJ, Wu M, Hudson MB, Nelson WB, and Powers SK**. Oxidative stress is required for mechanical ventilation-induced protease activation in the diaphragm. *J Appl Physiol* 108: 1376-1382.
60. **Yamazaki Y, Kamei Y, Sugita S, Akaike F, Kanai S, Miura S, Hirata Y, Troen BR, Kitamura T, Nishino I, Suganami T, Ezaki O, and Ogawa Y**. The

cathepsin L gene is a direct target of FOXO1 in skeletal muscle. *Biochem J* 427: 171-178, 2010.

61. **Zakynthinos SG, Vassilakopoulos T, and Roussos C**. The load of inspiratory muscles in patients needing mechanical ventilation. *Am J Respir Crit Care Med* 152: 1248-1255, 1995.

62. **Zolotukhin S, Potter M, Zolotukhin I, Sakai Y, Loiler S, Fraites TJ, Jr., Chiodo VA, Phillipsberg T, Muzyczka N, Hauswirth WW, Flotte TR, Byrne BJ, and Snyder RO**. Production and purification of serotype 1, 2, and 5 recombinant adeno-associated viral vectors. *Methods* 28: 158-167, 2002.

BIOGRAPHICAL SKETCH

Ashley Joslin Smuder was born in Naples, Florida. She earned a Bachelor of Science degree in exercise physiology from the University of Florida in 2006. Following graduation, she pursued a master's degree in exercise physiology and began her graduate work at the University of Florida in 2007 under the direction of Dr. Scott K. Powers. Ashley focused her studies on oxidative stress and proteolysis of the diaphragm during prolonged mechanical ventilation. She received her Master of Science degree in 2008. Ashley then began her doctoral work at the University of Florida again under the direction of Scott K. Powers. Ashley focused her studies on the mechanisms responsible for mechanical ventilation-induced diaphragm weakness. She received her PhD in 2012.